ANALISIS RIWAYAT RESPONS NONLINIER PADA SUBSTRUKTUR

F.X. Toha

July 12, 2022

SNI 1726 2019 ASCE 7-16

SNI

Standar Nasional Indonesia

SNI 1726:2019

Tata cara perencanaan ketahanan gempa untuk struktur bangunan gedung dan nongedung

BADAN STANDARDISASI NASIONAL

ICS 91.120.25; 91.080.01

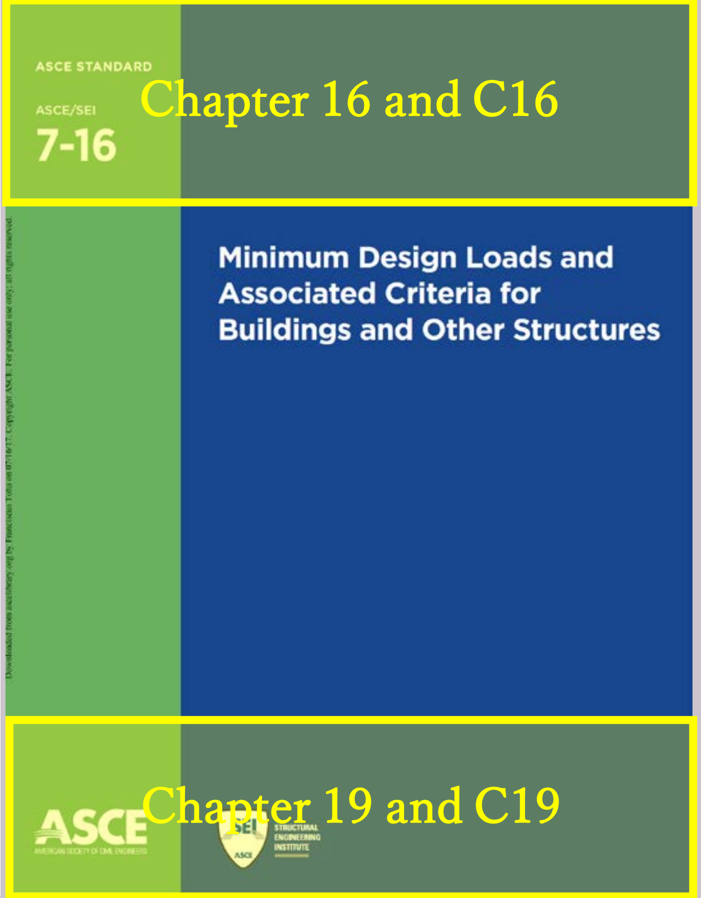

Kebutuhan RRNL:

1. Diijinkan ("*permitted*") (Pasal 11.1.1). "permitted when irregularity exists? Or, when a performance based analysis is desired?"
2. Harus didahului dengan RR Linier (Pasal 11.1.2), untuk memastikan bahwa strukturnya memenuhi semua kriteria kekuatan dan lainnya dalam Pasal 7.
3. Persyaratan tentang gerakan tanah dasar diatur secara rinci dalam Pasal 11, dan disampaikan oleh Ir. Sindhu Rudianto dalam acara sosialisasi ini.
4. Ada persyaratan dokumentasi, antara lain (khusus geoteknik): PSHA-SSRA, deskripsi pemodelan dan piranti lunak, data laboratorium, kriteria penerimaan, kriteria penerimaan bila terjadi deformasi > 150% dari yang diijinkan dalam Pasal 7.12

RRNL tanpa atau dengan Interaksi Tanah Struktur (SSI)?

- Praktisi Struktur Atas lebih memilih penjepitan di muka tanah atau kepala fondasi.
- Umumnya lebih aman, terutama untuk bangunan tinggi.
- SSI tidak mudah dilaksanakan dan konsensus masih subyektif.
- Berbahaya untuk bangunan dengan T rendah dan tanah sangat lunak

FEMA P-2091 (December 2020): A Practical Guide to Soil-Structure Interaction.

- Inertial SSI penting bila:

  $h'/(V_s T) > 0.1$

- Kinematik, lihat Pasal 14

Inersia Struktur Atas

Interaksi inersial umumnya menguntungkan bila $h'/(V_s T) < 0.1$, yakni untuk struktur fleksibel pada tanah keras/teguh. Merugikan bila strukturnya kaku dan tanahnya lunak

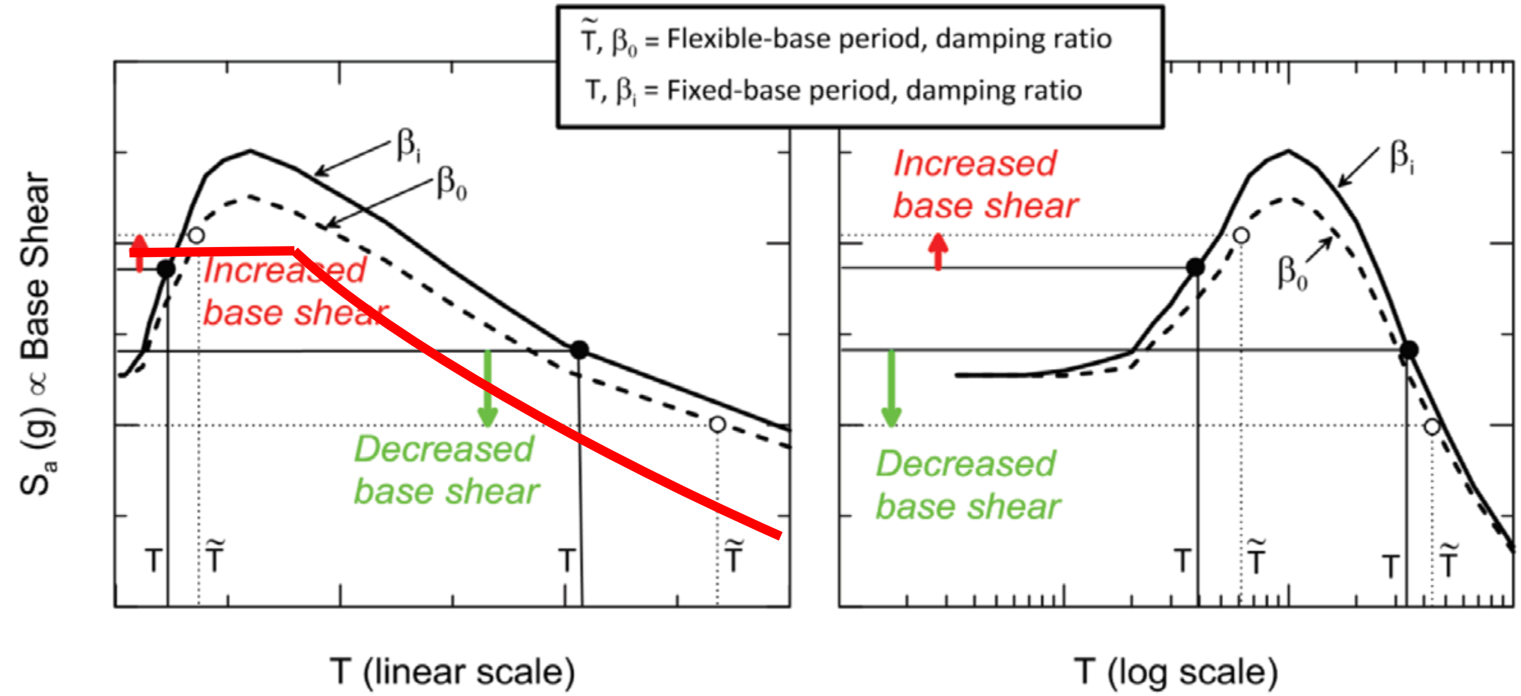

Figure 2-3 Illustration of inertial SSI effects on spectral acceleration (base shear) associated with period lengthening and change in damping.

<u>*Soil-Structure Interaction for Building Structures*</u>, NIST GCR 12-917-21, 2012

h' = effective structure height, measured from base of foundation to the center of mass of the fundamental mode (in ft). It can be approximated as 2/3 h_n, where h_n is the structure height as defined in ASCE/SEI 7-16 Section 11.2, plus the depth from grade to the bottom of the foundation.

v_s = the average effective shear wave velocity (ft/s) for site soil conditions, taken as the average value of velocity over the effective depth for foundation rotation determined using v_{so} and a velocity reduction factor from ASCE/SEI 7-16 Table 19.3-1 or a site-specific study. Calculation of v_{so} is discussed in Section 3.3 of this *Guide*.

T = fundamental mode of the structure assuming a fixed base at grade (in seconds). Calculation of T is discussed in Section 3.4 of this *Guide*.

3.3 Determining Average Effective Shear Wave Velocity

Site classification is based on the average low strain shear wave velocity, v_{so}, over the top 100 ft (or 30 m) of soil from grade. The average effective shear wave velocity, v_s, is a reduced value that accounts for the larger strains that occur during earthquake shaking. For the rule of thumb test, the depth of significance is not the same as that used for site soil classification. Calculation of the average low strain shear wave velocity over the effective depth for foundation rotation is determined as follows.

Step 1: Determine footing embedment depth, *e*.

The footing embedment depth, e, is the depth to from grade to the bottom of the footing.

Step 2: Determine the effective profile depth, z_p.

The effective profile depth per Equation 2-18c of NIST (2012a) is the parameter, z_p, as determined from the footing width and length as follows.

$$z_p = (B^3 L)^{0.25}$$

where:

B = overall foundation half width (ft). B is measured parallel to the direction of loading

L = overall foundation half width (ft). L is measured perpendicular to the direction of loading

Step 3: Determine the effective depth for foundation rotation, $e + z_p$.

The depth of interest for calculation of the average effective shear wave velocity is the effective depth for foundation rotation which is the sum of the foundation embedment depth and the effective profile depth or $e + z_p$.

Step 4: Determine the average low strain shear wave velocity, v_{so}, over the effective depth for foundation rotation.

Low strain shear wave velocity measurements are those measured for site classification. Typically, they are reported or graphed in layers. The average is determined using the same formula as ASCE/SEI 7-16 Equation 20.4-1.

$$v_{so} = \Sigma d_i / \Sigma(d_i / v_{si})$$

Step 6: Determine the average effective shear wave velocity, v_s.

The average effective shear wave velocity from the ground surface to depth $e + z_p$ is computed as follows:

$$v_s = [v_s / v_{so}]\,(v_{so})$$

where:

v_s = average effective shear wave velocity (ft/s) for site soil conditions

v_{so} = average low strain shear wave velocity (ft/s) for site soil conditions, computed as described in Step 4

$[v_s / v_{so}]$ = effective shear wave velocity ratio from ASCE/SEI 7-16 Table 19.3-1, as identified in Step 6.

Note that in ASCE/SEI 7-16 Section 19.3.3, the definition of v_s uses a depth measured from ground surface to depth e, not $e + z_p$.

3.4 Determining Fundamental Period of the Structure

The fundamental period of the structure can be obtained from a computer model or by using the approximate fundamental period from ASCE/SEI 7-16 Equation 12.8-7.

$$T = T_a = C_t\, h_n^x$$

where:

h_n = structure height as defined in ASCE/SEI 7-16 Section 11.2 plus depth of footing

C_t = coefficient from ASCE/SEI 7-16 Table 12.8-2 that depends on the structural system

x = coefficient from ASCE/SEI 7-16 Table 12.8-2 that depends on the structural system

RUJUKAN UMUM

Topik Pilihan tentang Beban Gempa pada Fondasi
sesuai
SNI 1726 2019 and SNI 8460 2017

SNI Gempa **SNI Geoteknik**

GEO – Talk XIII
4 Juni 2020
Web Seminar HATTI

F. X. Toha

Pemodelan Fondasi (Pasal 11.3.6)- ASCE 7-16 C16

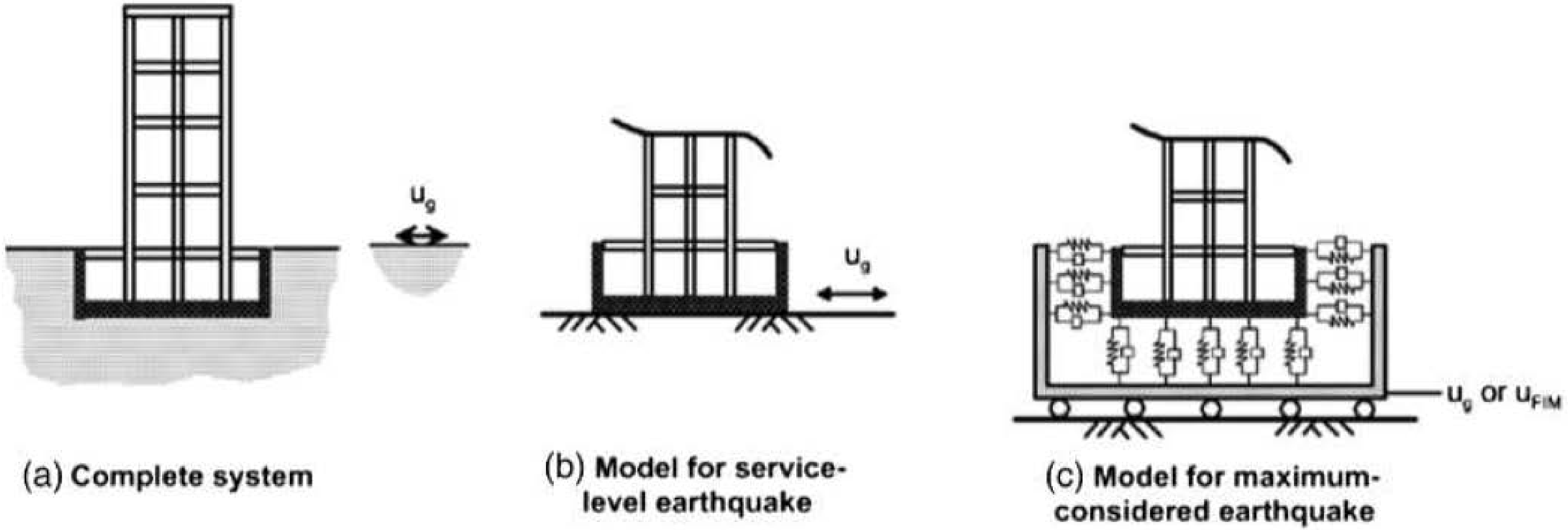

FIGURE C16.3-1 Illustration of the Method of Inputting Ground Motions into the Base of the Structural Model

Model analitik fondasi dalam analisis terhadap beban gempa:
Analisis interaksi dinamik tanah - fondasi – struktur (*Complete System*)

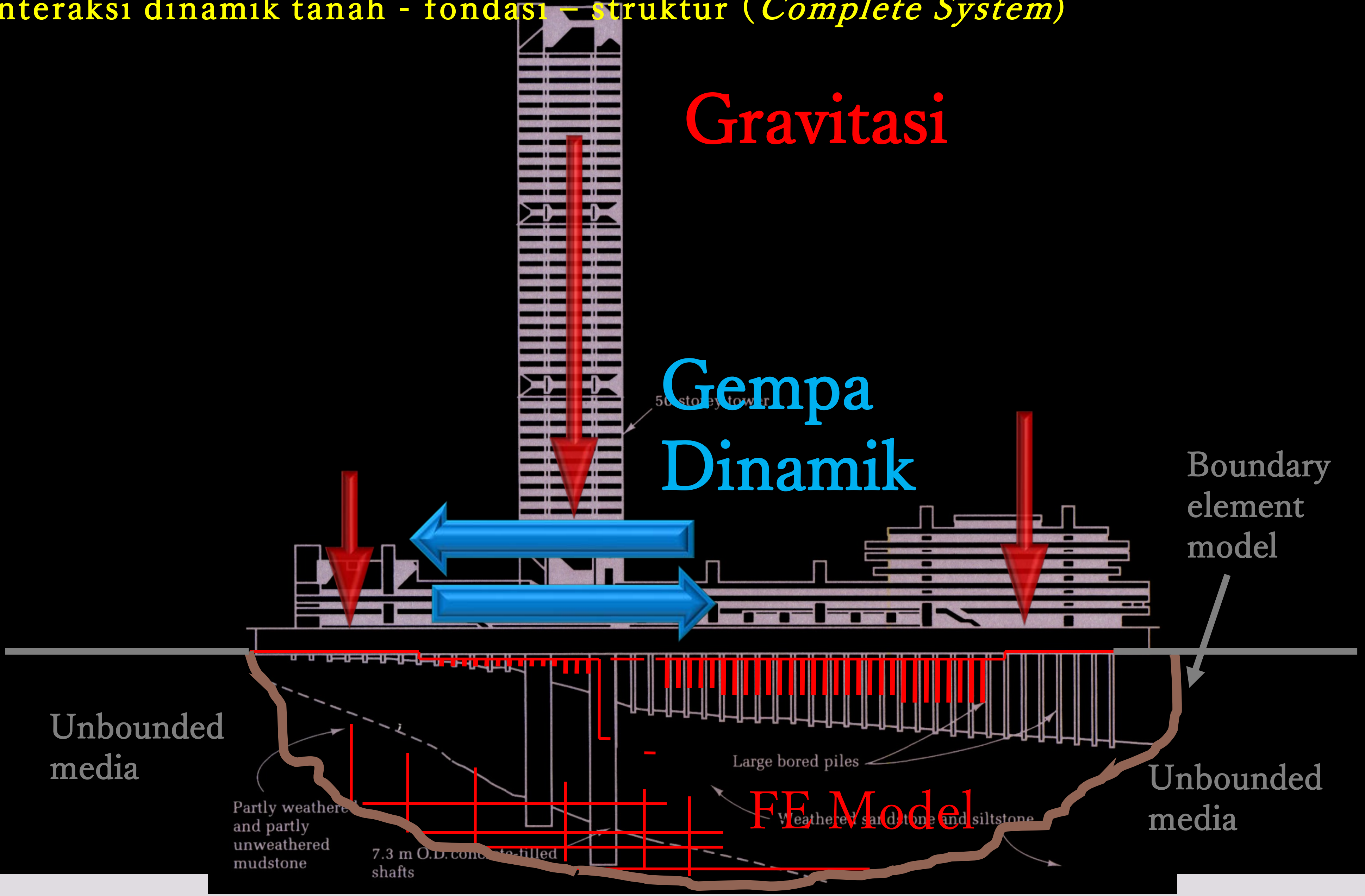

Geotechnical Model:

MODEL DASAR TERJEPIT (FIXED BASE MODEL)

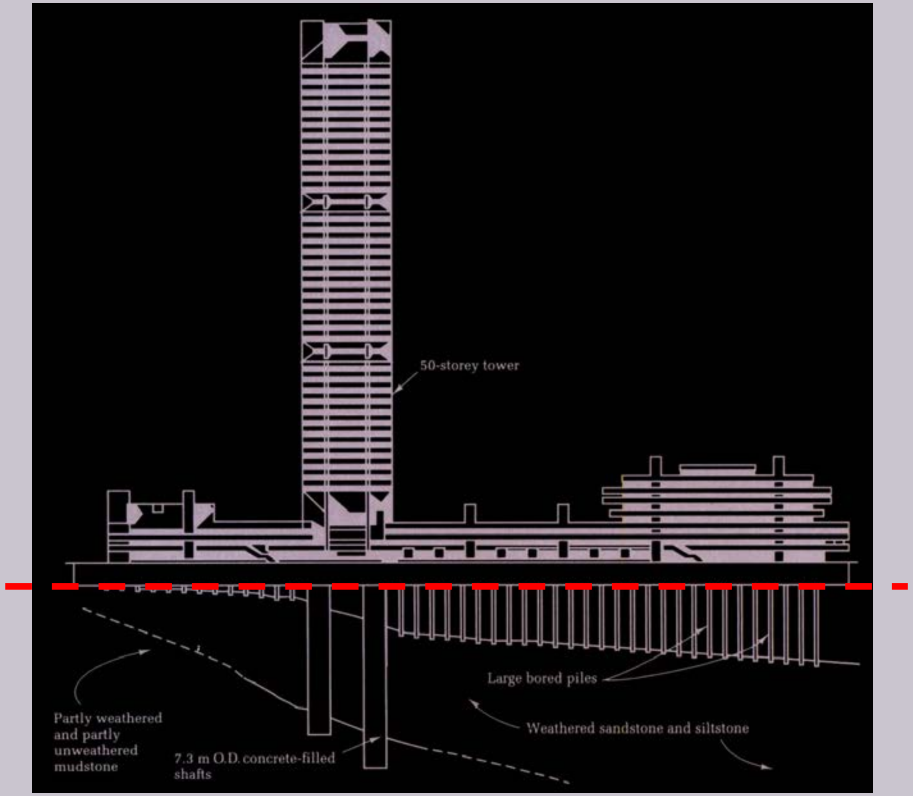

(BATHTUB MODEL)

NIST GCR 12-917-21 (2012): Soil Structure Interaction for Building Structures,: NEHRP

- Rigid Slab
- Flexible Foundations

Beban Gempa pada Fondasi:
Interaksi tanah – fondasi (beban struktur terjepit)

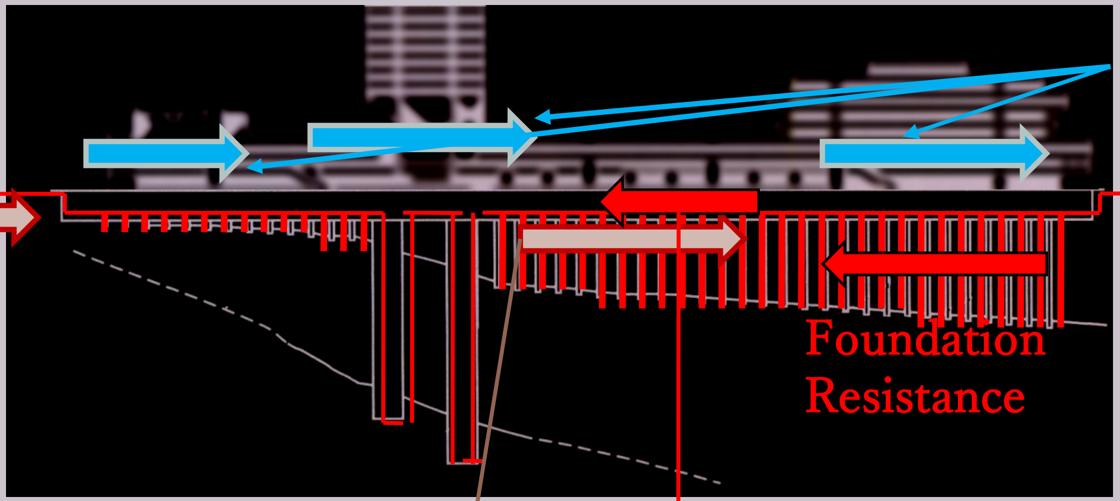

Beban Kinematik Basement dan Tiang:
(14.4), ASCE 7-16 14.2.3

Beban dari Tanah:
+ M&O (1930)
+ Seed & Whitman
+ Wood (1973)
+ Westergaard (1931)
+ Chwang and Housner (1977)
+ Sherif & Fang (1984)
+ Mikola & Sitar (2013)

+ Slopes
+ Lateral Spread

Beban Inersia Basement & Fondasi:
+ SNI 1726 2019 7.8.1.1
+ Historis SNI 1726 2002:
10 % x PGA;
merujuk ketentuan
Jepang

Ketentuan SNI 1726 2019 tentang sistem struktur atas terjepit di MT

<u>SNI 1726 2019 (7.2.3.1):</u>

- Bila $R_{SA} > R_f$: Gunakan $(R,\ C_d\ dan\ \Omega_0)_{SA}$ untuk bangunan atas, dan untuk bangunan bawah digunakan $(R,\ C_d\ dan\ \Omega_0)_f$ dan gaya struktur atas diperbesar dengan R_{SA} / R_f
- Bila $R_{SA} < R_f$: Gunakan $(R,\ C_d\ dan\ \Omega_0)_{SA}$ untuk bangunan atas dan bawah.

<u>SNI 1726 2019 (7.2.3.2):</u>

- Asumsi penjepitan diperkenankan bila kekakuan bangunan bawah ≥ 10 kekakuan bangunan atas.
- T_{sistem} dibatasi maksimum 1.1 x $T_{terjepit}$
- $F_f \geq 1.5\ (R/\rho)_{SA} / (R/\rho)_f\, F_{SA}$ di mana $(R/\rho)_{SA} / (R/\rho)_f \geq 1.0$

ASCE 7-16 12.2.3.2 = 1.0

NIST GCR 12-917-21 (2012): Soil Structure Interaction for Building Structures,: NEHRP

Rigid Base Procedures

FEMA 440-2005 - Chapter 8

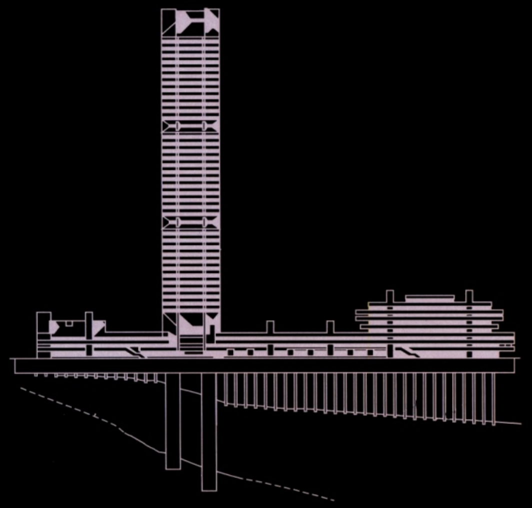

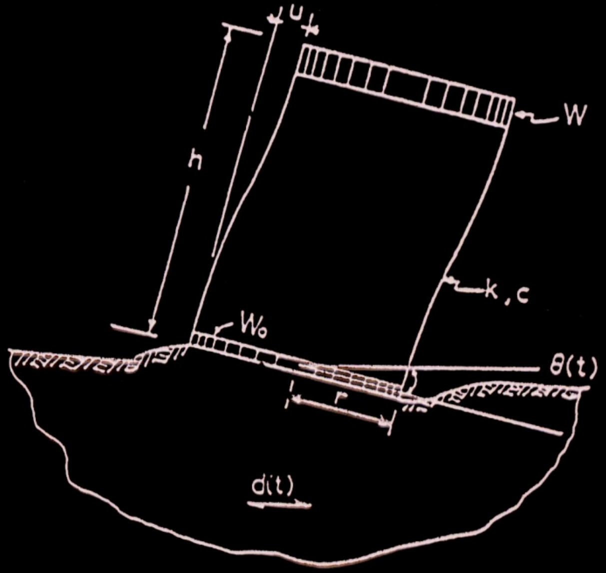

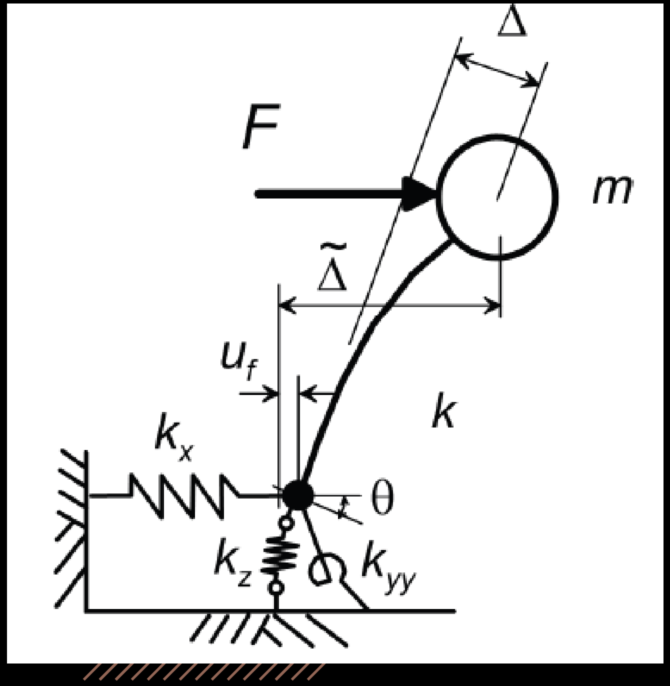

Table 2-2a Elastic Solutions for Static Stiffness of Rigid Footings at the Ground Surface

Degree of Freedom	Pais and Kausel (1988)	Gazetas (1991); Mylonakis et al. (2006)
Translation along z-axis	$K_{z,\,sur} = \dfrac{GB}{1-\nu}\left[3.1\left(\dfrac{L}{B}\right)^{0.75} + 1.6\right]$	$K_{z,\,sur} = \dfrac{2GL}{1-\nu}\left[0.73 + 1.54\left(\dfrac{B}{L}\right)^{0.75}\right]$
Translation along y-axis	$K_{y,\,sur} = \dfrac{GB}{2-\nu}\left[6.8\left(\dfrac{L}{B}\right)^{0.65} + 0.8\left(\dfrac{L}{B}\right) + 1.6\right]$	$K_{y,\,sur} = \dfrac{2GL}{2-\nu}\left[2 + 2.5\left(\dfrac{B}{L}\right)^{0.85}\right]$
Translation along x-axis	$K_{x,\,sur} = \dfrac{GB}{2-\nu}\left[6.8\left(\dfrac{L}{B}\right)^{0.65} + 2.4\right]$	$K_{x,\,sur} = K_{y,\,sur} - \dfrac{0.2}{0.75-\nu}GL\left(1 - \dfrac{B}{L}\right)$
Torsion about z-axis	$K_{zz,\,sur} = GB^3\left[4.25\left(\dfrac{L}{B}\right)^{2.45} + 4.06\right]$	$K_{zz,\,sur} = GJ_t^{0.75}\left[4 + 11\left(1 - \dfrac{B}{L}\right)^{10}\right]$
Rocking about y-axis	$K_{yy,\,sur} = \dfrac{GB^3}{1-\nu}\left[3.73\left(\dfrac{L}{B}\right)^{2.4} + 0.27\right]$	$K_{yy,\,sur} = \dfrac{G}{1-\nu}\left(I_y\right)^{0.75}\left[3\left(\dfrac{L}{B}\right)^{0.15}\right]$
Rocking about x-axis	$K_{xx,\,sur} = \dfrac{GB^3}{1-\nu}\left[3.2\left(\dfrac{L}{B}\right) + 0.8\right]$	$K_{xx,\,sur} = \dfrac{G}{1-\nu}\left(I_x\right)^{0.75}\left(\dfrac{L}{B}\right)^{0.25}\left[2.4 + 0.5\left(\dfrac{B}{L}\right)\right]$

Notes:

Axes should be oriented such that $L \geq B$.

I_i = area moment of inertia of soil-foundation contact, i denotes which axis to take the surface around.

$J_t = I_x + I_y$ polar moment of inertia of soil-foundation contact surface.

G = shear modulus (reduced for large strain effects, e.g., Table 2-1).

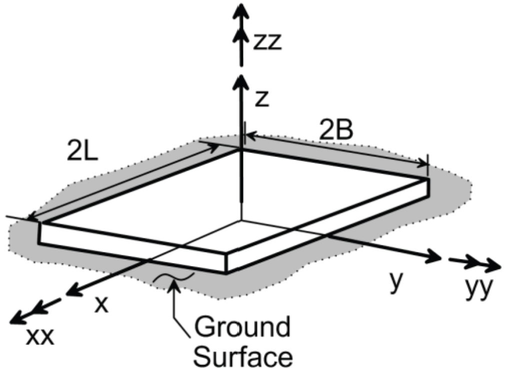

Table 2-2b Embedment Correction Factors for Static Stiffness of Rigid Footings

Degree of Freedom	Pais and Kausel (1988)	Gazetas (1991); Mylonakis et al. (2006)
Translation along z-axis	$\eta_z = \left[1.0 + \left(0.25 + \frac{0.25}{L/B}\right)\left(\frac{D}{B}\right)^{0.8}\right]$	$\eta_z = \left[1 + \frac{D}{21B}\left(1 + 1.3\frac{B}{L}\right)\right]\left[1 + 0.2\left(\frac{A_w}{4BL}\right)^{2/3}\right]$
Translation along y-axis	$\eta_y = \left[1.0 + \left(0.33 + \frac{1.34}{1 + L/B}\right)\left(\frac{D}{B}\right)^{0.8}\right]$	$\eta_y = \left(1 + 0.15\sqrt{\frac{D}{B}}\right)\left[1 + 0.52\left(\frac{z_w A_w}{BL^2}\right)^{0.4}\right]$
Translation along x-axis	$\eta_x \approx \eta_y$	Same equation as for η_y, but A_w term changes for $B \neq L$
Torsion about z-axis	$\eta_{zz} = \left[1 + \left(1.3 + \frac{1.32}{L/B}\right)\left(\frac{D}{B}\right)^{0.9}\right]$	$\eta_{zz} = 1 + 1.4\left(1 + \frac{B}{L}\right)\left(\frac{d_w}{B}\right)^{0.9}$
Rocking about y-axis	$\eta_{yy} = \left[1.0 + \frac{D}{B} + \left(\frac{1.6}{0.35 + (L/B)^4}\right)\left(\frac{D}{B}\right)^2\right]$	$\eta_{yy} = 1 + 0.92\left(\frac{d_w}{B}\right)^{0.6}\left[1.5 + \left(\frac{d_w}{D}\right)^{1.9}\left(\frac{B}{L}\right)^{-0.6}\right]$
Rocking about x-axis	$\eta_{xx} = \left[1.0 + \frac{D}{B} + \left(\frac{1.6}{0.35 + L/B}\right)\left(\frac{D}{B}\right)^2\right]$	$\eta_{xx} = 1 + 1.26\frac{d_w}{B}\left[1 + \frac{d_w}{B}\left(\frac{d_w}{D}\right)^{-0.2}\sqrt{\frac{B}{L}}\right]$

Notes:

d_w = height of effective side wall contact (may be less than total foundation height)

z_w = depth to centroid of effective sidewall contact

A_w = sidewall-solid contact area, for constant effective contact height, d_w, along perimeter.

For each degree of freedom, calculate $K_{emb} = \eta K_{sur}$

Coupling Terms: $K_{emb,rx} = \left(\frac{D}{3}\right)K_{emb,x}$

$K_{emb,ry} = \left(\frac{D}{3}\right)K_{emb,y}$

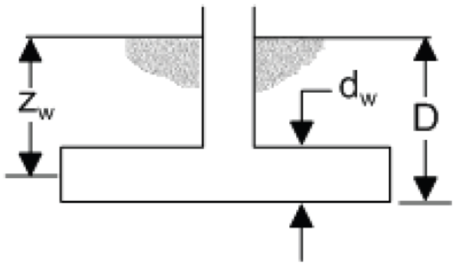

Table 2-3a Dynamic Stiffness Modifiers and Radiation Damping Ratios for Rigid Footings (adapted from Pais and Kausel, 1988)

Degree of Freedom	Surface Stiffness Modifiers	Radiation Damping
Translation along z-axis	$\alpha_z = 1.0 - \left[\dfrac{\left(0.4 + \dfrac{0.2}{L/B}\right) a_0^2}{\left(\dfrac{10}{1+3(L/B-1)}\right) + a_0^2} \right]$	$\beta_z = \left[\dfrac{4\psi(L/B)}{(K_{z,sur}/GB)}\right]\left[\dfrac{a_0}{2\alpha_z}\right]$
Translation along y-axis	$\alpha_y = 1.0$	$\beta_y = \left[\dfrac{4(L/B)}{(K_{y,sur}/GB)}\right]\left[\dfrac{a_0}{2\alpha_y}\right]$
Translation along x-axis	$\alpha_x = 1.0$	$\beta_x = \left[\dfrac{4(L/B)}{(K_{x,sur}/GB)}\right]\left[\dfrac{a_0}{2\alpha_x}\right]$
Torsion about z-axis	$\alpha_{zz} = 1.0 - \left[\dfrac{\left(0.33 - 0.03\sqrt{L/B-1}\right) a_0^2}{\left(\dfrac{0.8}{1+0.33(L/B-1)}\right) + a_0^2} \right]$	$\beta_{zz} = \left[\dfrac{(4/3)\left[(L/B)^3 + (L/B)\right] a_0^2}{\left(K_{zz,sur}/GB^3\right)\left[\left(\dfrac{1.4}{1+3(L/B-1)^{0.7}}\right) + a_0^2\right]} \right]\left[\dfrac{a_0}{2\alpha_{zz}}\right]$
Rocking about y-axis	$\alpha_{yy} = 1.0 - \left[\dfrac{0.55 a_0^2}{\left(0.6 + \dfrac{1.4}{(L/B)^3}\right) + a_0^2} \right]$	$\beta_{yy} = \left[\dfrac{(4\psi/3)(L/B)^3 a_0^2}{\left(\dfrac{K_{yy,sur}}{GB^3}\right)\left[\left(\dfrac{1.8}{1+1.75(L/B-1)}\right) + a_0^2\right]} \right]\left[\dfrac{a_0}{2\alpha_{yy}}\right]$
Rocking about x-axis	$\alpha_{xx} = 1.0 - \left[\dfrac{\left(0.55 + 0.01\sqrt{L/B-1}\right) a_0^2}{\left(2.4 - \dfrac{0.4}{(L/B)^3}\right) + a_0^2} \right]$	$\beta_{xx} = \left[\dfrac{(4\psi/3)(L/B) a_0^2}{\left(K_{xx,sur}/GB^3\right)\left[\left(2.2 - \dfrac{0.4}{(L/B)^3}\right) + a_0^2\right]} \right]\left[\dfrac{a_0}{2\alpha_{xx}}\right]$

Notes: Orient axes such that $L \geq B$.

Soil hysteretic damping, β_s, is additive to foundation radiation damping, β_i.

$a_0 = \omega B / V_s$; $\psi = \sqrt{2(1-\nu)/(1-2\nu)}$; $\psi \leq 2.5$

Table 2-3b Dynamic Stiffness Modifiers and Radiation Damping Ratios for Embedded Footings (adapted from Pais and Kausel, 1988)

Degree of Freedom	Radiation Damping
Translation along z-axis	$\beta_z = \left[\dfrac{4\left[\psi(L/B)+(D/B)(1+L/B)\right]}{\left(K_{z,emb}/GB\right)}\right]\left[\dfrac{a_0}{2\alpha_z}\right]$
Translation along y-axis	$\beta_y = \left[\dfrac{4\left[L/B+(D/B)(1+\psi L/B)\right]}{\left(K_{y,emb}/GB\right)}\right]\left[\dfrac{a_0}{2\alpha_y}\right]$
Translation along x-axis	$\beta_x = \left[\dfrac{4\left[L/B+(D/B)(\psi+L/B)\right]}{\left(K_{x,emb}/GB\right)}\right]\left[\dfrac{a_0}{2\alpha_x}\right]$
Torsion about z-axis	$\beta_{zz} = \left[\dfrac{(4/3)\left[3(L/B)(D/B)+\psi(L/B)^3(D/B)+3(L/B)^2(D/B)+\psi(D/B)+(L/B)^3+(L/B)\right]a_0^2}{\left(\dfrac{K_{zz,emb}}{GB^3}\right)\left[\left(\dfrac{1.4}{1+3(L/B-1)^{0.7}}\right)+a_0^2\right]}\right]\left[\dfrac{a_0}{2\alpha_{zz}}\right]$
Rocking about y-axis	$\beta_{yy} = \left[\dfrac{(4/3)\left[\left(\dfrac{L}{B}\right)^3\left(\dfrac{D}{B}\right)+\psi\left(\dfrac{D}{B}\right)^3\left(\dfrac{L}{B}\right)+\left(\dfrac{D}{B}\right)^3+3\left(\dfrac{D}{B}\right)\left(\dfrac{L}{B}\right)^2+\psi\left(\dfrac{L}{B}\right)^3\right]a_0^2}{\left(\dfrac{K_{yy,emb}}{GB^3}\right)\left[\left(\dfrac{1.8}{1+1.75(L/B-1)}\right)+a_0^2\right]}+\dfrac{\left(\dfrac{4}{3}\right)\left(\dfrac{L}{B}+\psi\right)\left(\dfrac{D}{B}\right)^3}{\left(\dfrac{K_{yy,emb}}{GB^3}\right)}\right]\left[\dfrac{a_0}{2\alpha_{yy}}\right]$
Rocking about x-axis	$\beta_{xx} = \left[\dfrac{(4/3)\left[\left(\dfrac{D}{B}\right)+\left(\dfrac{D}{B}\right)^3+\psi\left(\dfrac{L}{B}\right)\left(\dfrac{D}{B}\right)^3+3\left(\dfrac{D}{B}\right)\left(\dfrac{L}{B}\right)+\psi\left(\dfrac{L}{B}\right)\right]a_0^2}{\left(\dfrac{K_{xx,emb}}{GB^3}\right)\left[\left(\dfrac{1.8}{1+1.75(L/B-1)}\right)+a_0^2\right]}+\dfrac{\left(\dfrac{4}{3}\right)\left(\psi\dfrac{L}{B}+1\right)\left(\dfrac{D}{B}\right)^3}{\left(\dfrac{K_{xx,emb}}{GB^3}\right)}\right]\left[\dfrac{a_0}{2\alpha_{xx}}\right]$
Notes:	Soil hysteretic damping, β_s, is additive to foundation radiation damping, β_i. $\alpha_{emb} = \alpha_{sur}$; from Table 2-3a $a_0 = \omega B / V_s$; $\psi = \sqrt{2(1-\nu)/(1-2\nu)}$; $\psi \le 2.5$

Flexible Base

$$\Psi = \frac{G r_f^3}{\left(E_f t_f^3 / \left(12(1-\nu_f^2)\right)\right)}$$

$$k_z^i = \frac{k_z}{4BL}$$

$$c_z^i = \frac{c_z}{4BL}$$

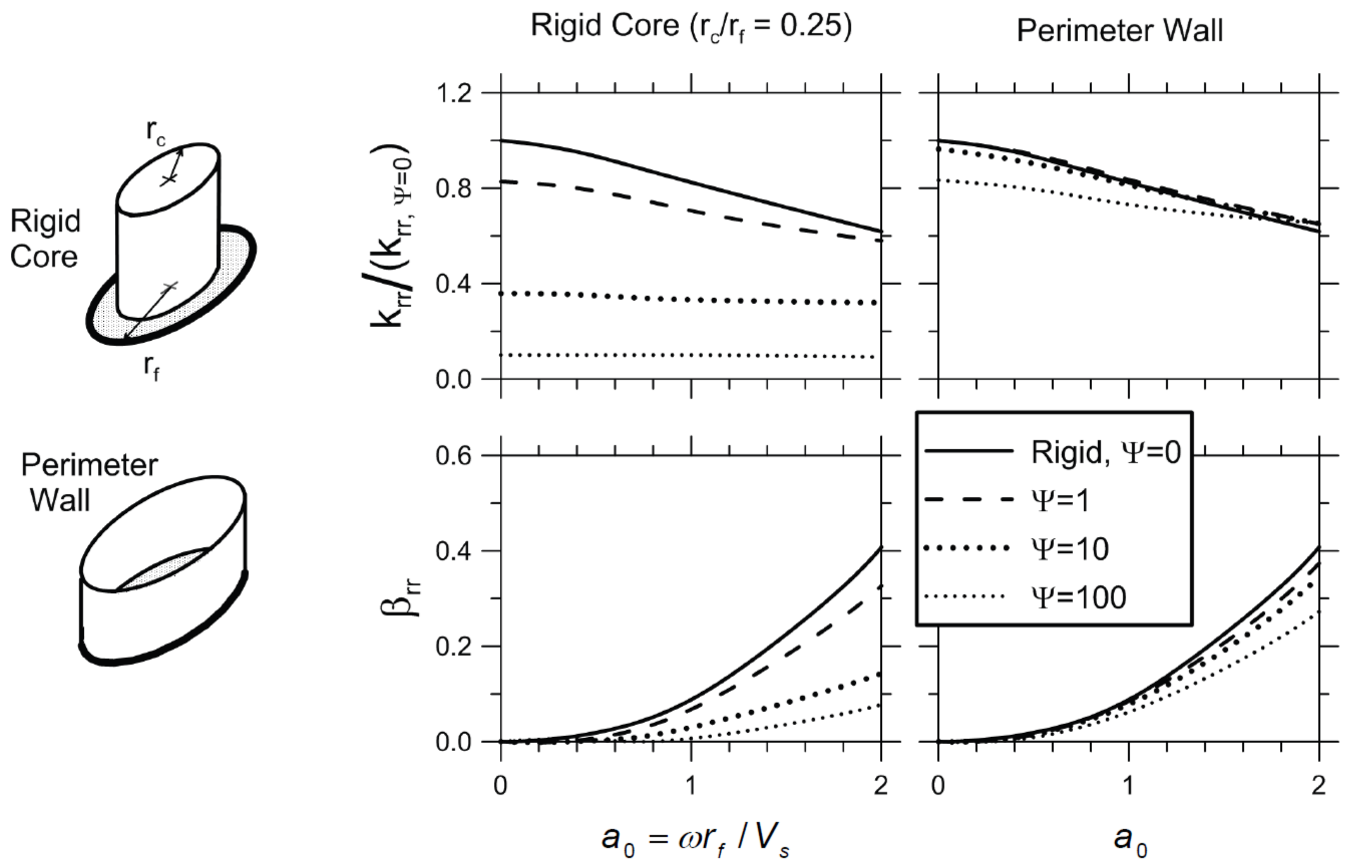

Figure 2-7 Effect of flexible foundation elements on rotational stiffness (k_{rr}) and rotational radiation damping ratio (β_{rr}) for circular foundations supporting a rigid core (Iguchi and Luco, 1982) and flexible perimeter walls (Liou and Huang, 1994).

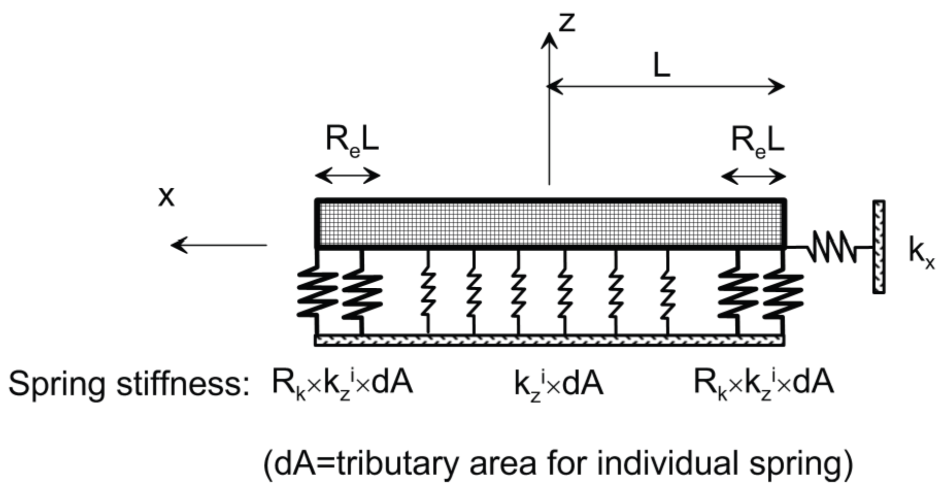

Figure 2-8 Vertical spring distribution used to reproduce total rotational stiffness k_{yy}. A comparable geometry can be shown in the y-z plane (using foundation dimension 2B) to reproduce k_{xx}.

More generally, the increase in spring stiffness, R_k, can be calculated as a function of foundation end length ratio, R_e, as:

$$Rocking(yy):\quad R_{k,yy}=\frac{\left(\dfrac{3k_{yy}}{4k_z^iBL^3}\right)-(1-R_e)^3}{1-(1-R_e)^3} \qquad (2\text{-}21a)$$

$$Rocking(xx):\quad R_{k,xx}=\frac{\left(\dfrac{3k_{xx}}{4k_z^iB^3L}\right)-(1-R_e)^3}{1-(1-R_e)^3} \qquad (2\text{-}21b)$$

To correct for overestimation of rotational damping, the relative stiffness intensities and distribution are used (based on the stiffness factor R_k and end length ratio R_e), but dashpot intensities over the full length and width of the foundation are scaled down by a factor, R_c, computed as:

$$Rocking(yy):\quad R_{c,yy}=\frac{\dfrac{3c_{yy}}{4c_z^iBL^3}}{R_{k,yy}\left(1-(1-R_e)^3\right)+(1-R_e)^3} \qquad (2\text{-}21c)$$

$$Rocking(xx):\quad R_{c,xx}=\frac{\dfrac{3c_{xx}}{4c_z^iB^3L}}{R_{k,xx}\left(1-(1-R_e)^3\right)+(1-R_e)^3} \qquad (2\text{-}21d)$$

$$R_e = 0.3 \text{ to } 0.5$$

Piles

Table 2-4a Equations for Static Stiffness of Single Piles

Degree of Freedom	Surface Stiffness Modifiers	Reference
Translation along x-axis	$\chi_x = \frac{1}{2}\pi^{1/4}\delta_x^{\ 3/4}\left(\frac{E_p}{E_s}\right)^{1/4}$	Poulos and Davis (1980) Scott (1981), Mylonakis (1995)
	$\delta_x = 2\left(\frac{E_p}{E_s}\right)^{-3/40}$	Dobry et al. (1982) Syngros (2004)
	$\left.\begin{aligned} w_{px} &= 1/4 \\ w_{sx} &= 3/4 \\ w_{bx} &= 0 \end{aligned}\right\} \text{Long pile } (L_p / d > L_{active})$	Dobry et al. (1982) Mylonakis (1995) Mylonakis and Roumbas (2001)
Translation along z-axis	$\chi_z = \left(\frac{\pi\delta_z}{2}\right)^{1/2}\left(\frac{E_p}{E_s}\right)^{1/2}\frac{\Omega + \tanh(\lambda L_p)}{1 + \Omega\tanh(\lambda L_p)}$	Randolph and Wroth (1978) Scott (1981)
	$\Omega = \frac{2}{\left(\sqrt{\pi\delta_z}\right)\left(1-\nu^2\right)}\left(\frac{E_p}{E_s}\right)^{-1/2}$ $\lambda L_p = \left(\frac{4\delta_z}{\pi}\right)^{\frac{1}{2}}\left(\frac{E_p}{E_s}\right)^{-\frac{1}{2}}\left(\frac{L_p}{d}\right)$	Mylonakis and Gatezas (1998), Randolph (2003), Salgado (2008)
	$\delta_z = 0.6 \ ; \ \left(L_p / d > 10, \ E_p / E_s > 100\right)$	Blaney et al. (1975) Roesset (1980) Thomas (1980)
	$w_{pz} = 1 - \left(w_{sz} + w_{bz}\right)$ $w_{sz} = \frac{-2\left[\left(\lambda L_p\right)\left(\Omega^2 - 1\right) + \Omega\right] + 2\Omega\cosh\left(2\lambda L_p\right) + \left(1+\Omega^2\right)\sinh\left(2\lambda L_p\right)}{4\cosh^2\left(\lambda L_p\right)\left[\Omega + \tanh\left(\lambda L_p\right)\right]\left[1 + \Omega\tanh\left(\lambda L_p\right)\right]}$ $w_{bz} = \frac{2\Omega}{2\Omega\cosh\left(\lambda L_p\right)\left(1+\Omega^2\right)\sinh\left(\lambda L_p\right)}$	

Degree of Freedom	Damping Ratio	Reference
Translation along x-axis	$\beta_x^p = \frac{1}{4}\beta_p + \frac{3}{4}\beta_s + \frac{3}{4}\beta_{rx}$	Dobry et al. (1982) Mylonakis and Roumbas (2001)
	$\beta_{rx} = \left[\frac{3}{2\alpha_x(1+\nu)\delta_x}\right]\left(a_o^p\right)^{3/4}$	Gazetas and Dobry (1984a,b)
Translation along z-axis	$\beta_z^p = w_{pz}\beta_p + \left(w_{sz} + w_{pz}\right)\beta_s + \beta_{rz}$	Mylonakis (2011)
	$\beta_{rz} = \frac{1}{\alpha_z^p}\left[w_{sz}\frac{1.2\pi}{4(1+\nu)\delta_z}\left(a_o^p\right)^{3/4} + w_{bz}0.21a_o^p\right]$	Gazetas and Dobry (1984b)

Pile Groups

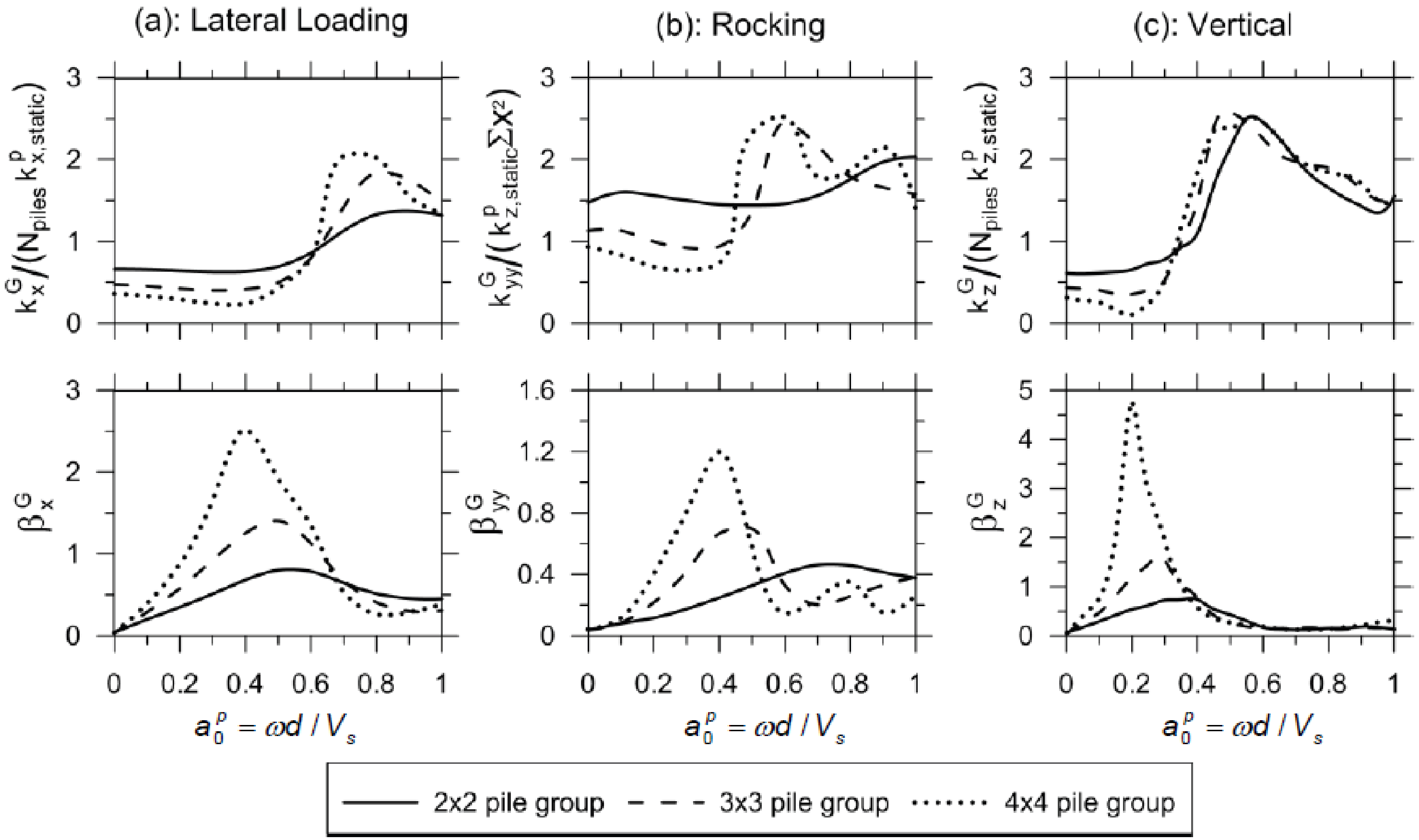

Figure 2-11 Plots of pile group efficiency factors and damping ratios versus dimensionless frequency for square pile groups for: (a) lateral loading at head of pile group under zero cap rotation; (b) moment at head of pile group, introducing rocking under zero cap translation; and (c) vertical loading at head of pile group. Lateral and rocking results are for E_p/E_s = 1000, L_p/d = 20, ρ_p/ρ_s = 1.3, ν=0.4, (pile spacing)/d = 5, β_p = 0, and β_s = 0.05. Vertical resutls are for E_p/E_s = 100, L_p/d = 15, ρ_p/ρ_s = 1.4, ν = 0.4, (pile spacing)/d = 5, β_p = 0, and β_s = 0.05.

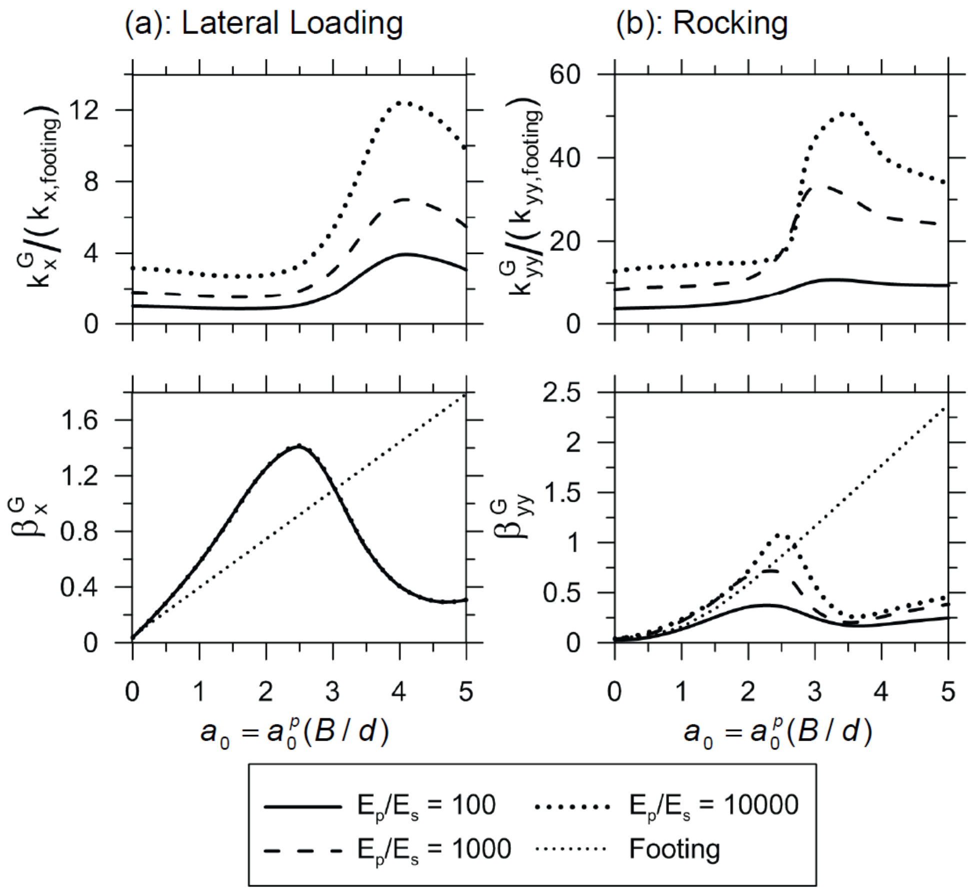

Figure 2-12 Comparison between the impedance (stiffness and damping ratio) of a 3x3 pile group and the impedance of a footing with equivalent dimensions for: (a) lateral loading at head of pile group; and (b) moment at head of pile group, introducing rocking. Results are for L_p/d = 20, ρ_p/ρ_s = 1.3, ν =0.4, (pile spacing)/d = 5, β_p = 0, and β_s = 0.05.

ITS Nonlinear untuk RRNL

Sumber Non Linieritas:

- Pelelehan Elemen Struktur Atas Penahan Gempa
- Pelelehan Tanah, diakibatkan kehilangan kuat geser (likuifaksi dan pelunakan siklik).
- Pembentukan celah (*gapping*) antara tanah dan stuktur fondasi, antara lain akibat *base uplift*, pemisahan dinding dari tanah.
- Pelelehan elemen struktur fondasi.

Praktik/Riset SSI

- Struktur non linier, tanah linier atau linier ekivalen
- Tanah non linier, struktur linier.

Pemodelan basemen (FEMA 2091 2020)

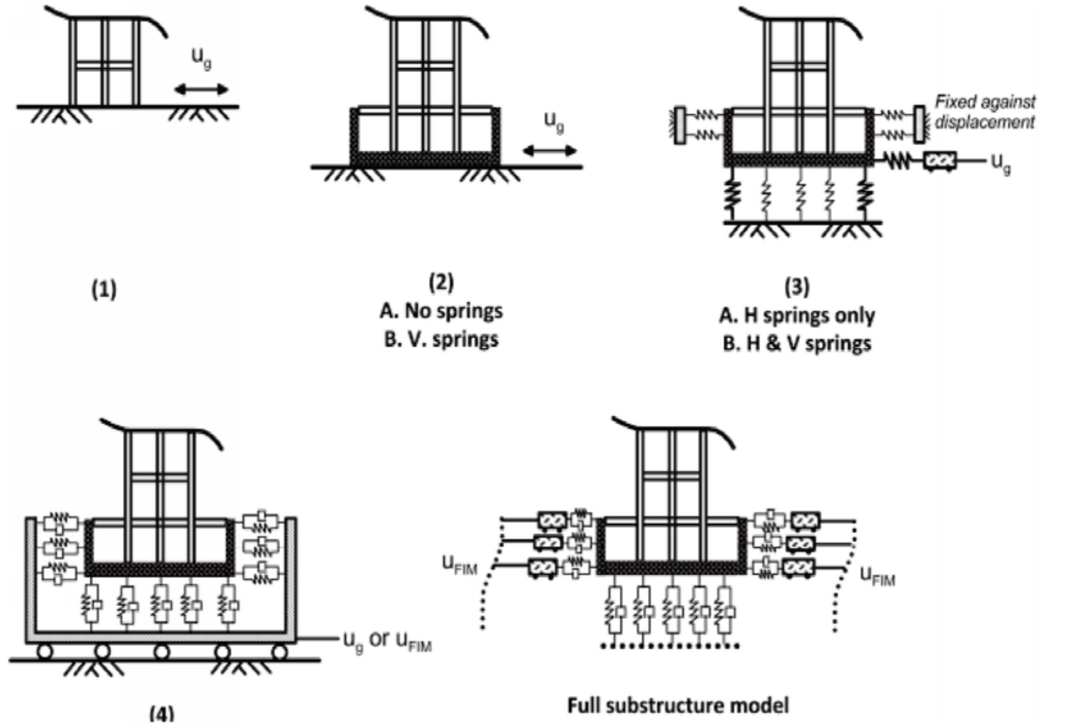

Figure 9-2 Modeling approaches for buildings with basements [from Figure 6-2 in NIST (2012a)]. u_g represents the free field motion, and u_{FIM} represents the foundation input motion. In Model 3 and the full substructure model, the little boxcars are sliders to which the free-field motion is applied. They do not have mass. The mass of the soil is included in the calculation of the free-field motions (and, as applicable, its depth-dependence).

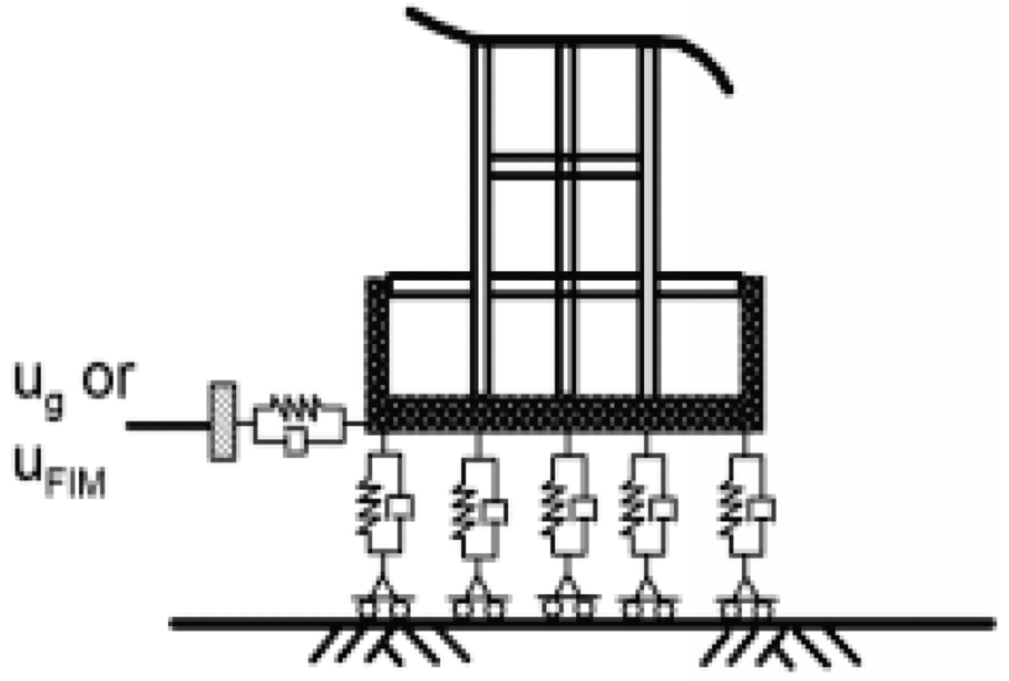

A Practical Guide to Soil-Structure Interaction, FEMA P-2091, December 2020

Model 1

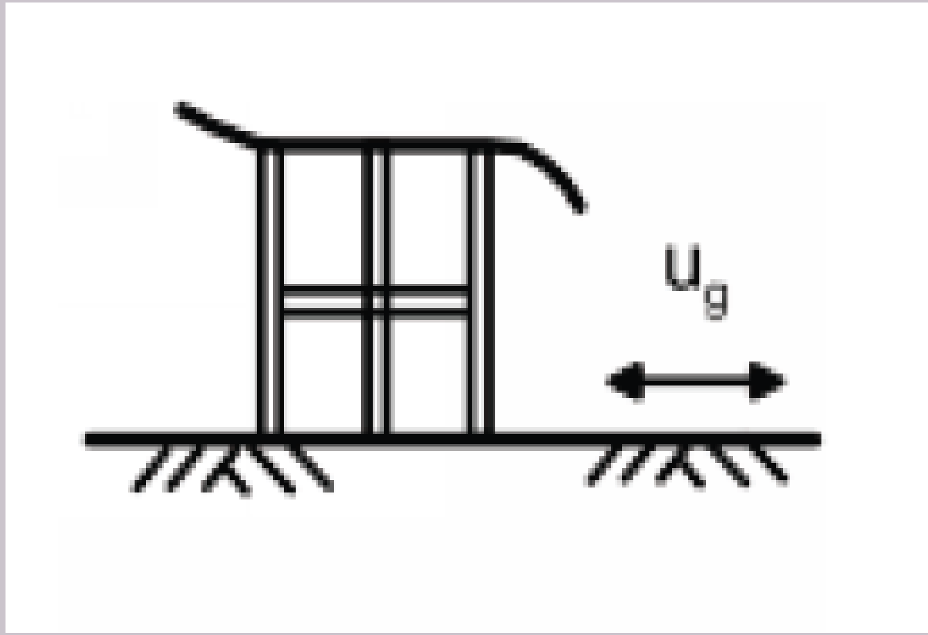

- Model ini paling sering digunakan
- Cocok untuk struktur atas *moment frame* dan *braced frame*. Tidak cocok untuk bangunan dengan dinding geser.

Model 2

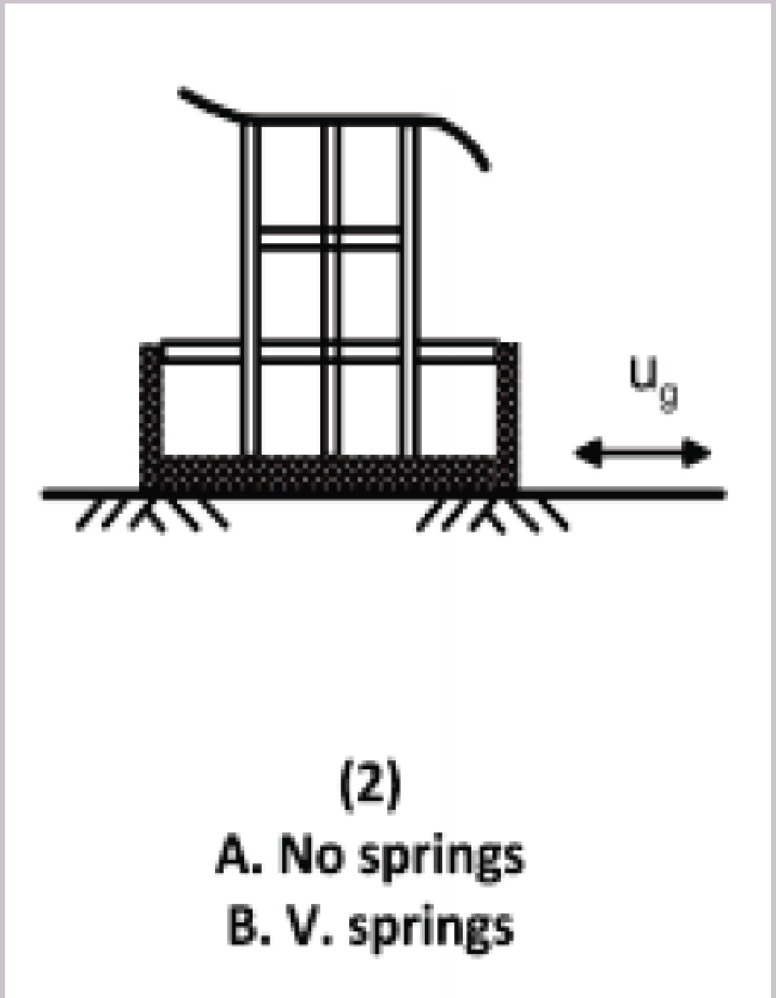

- Didasari pemikiran bahwa timbulnya reaksi (passive)pada dinding basemen butuh deformasi yang besar.
- Model 2A sering digunakan untuk preliminary design
- Model 2B dan Model 1 sering digunakan sebagai batasan dalam desain.

Model 3

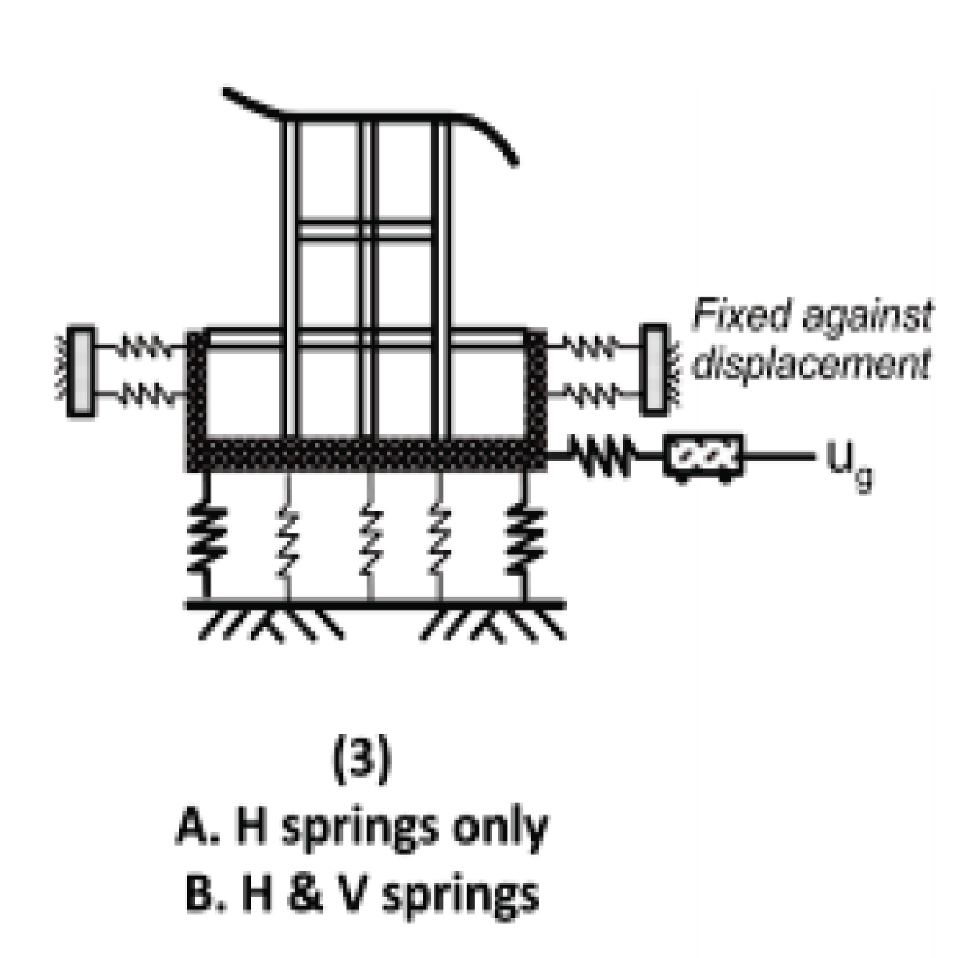

- Pengaruh tanah di samping dinding disertakan, dan percepatan tanah pada dasar basemen.
- Umumnya digunakan untuk *push over analysis.*
- Model ini agak jarang digunakan

Model 4

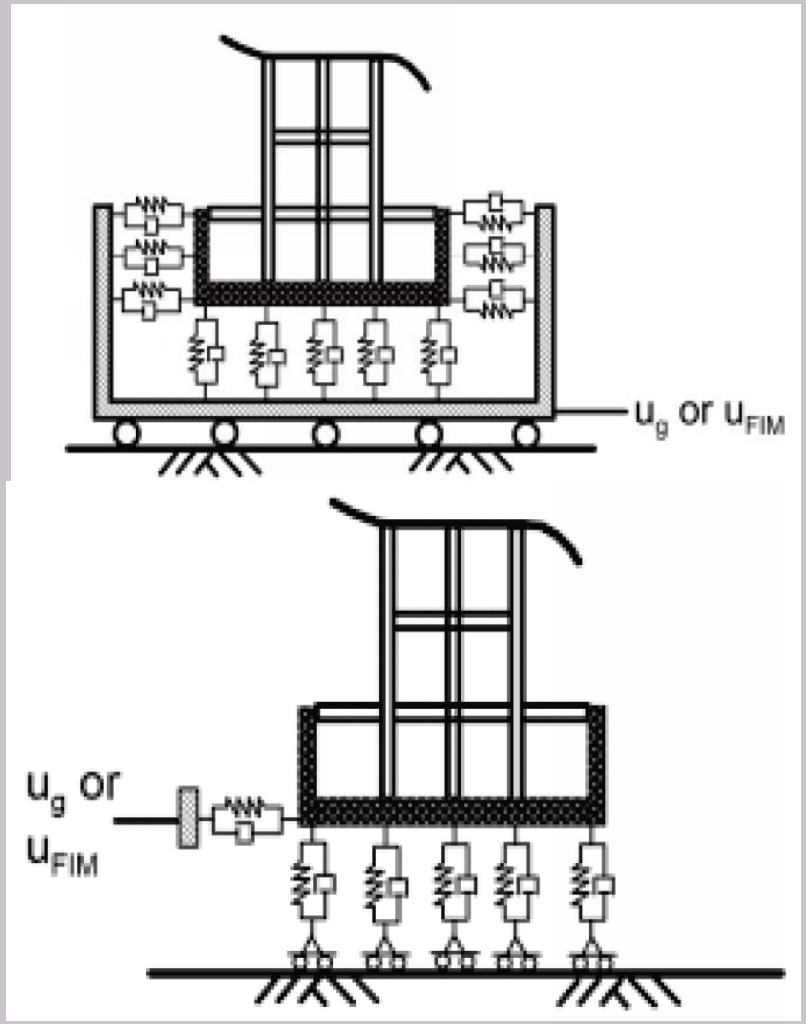

- Model tanah disambung ke bak kaku (*bathtub*), dan gempa bekerja pada bak kaku.
- Walaupun model ini dianjurkan di PEER 2017, model ini jarang digunakan praktisi.
- Model ini bisa disederhanakan seperti yang di bawahnya.

Model Substruktur Penuh (*Baseline Model*)

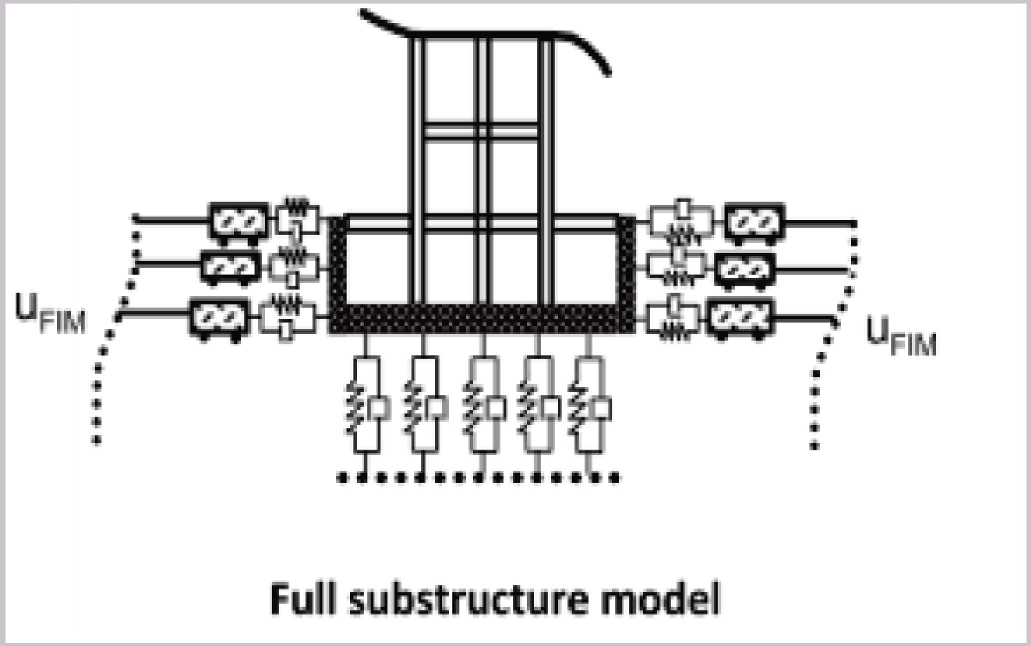

- Model ini dilengkapi dengan pemodelan pegas dan peredam di samping dan di bawah, dan gempa bekerja pada batas samping dan bawah,
- Model ini belum tercatat digunakan dalam praktik (FEMA 2090 2020).

SNI 1726 2019 Bab 14 (Interaksi Tanah Struktur) – ITS Kinematik

- Pengaruh Perataan Plat Dasar (*Base Slab Averaging*): (RRS_{bsa} x RRS_e)

$$RRS_{bsa} = 0{,}25 + 0{,}75 \times \left\{\frac{1}{b_0^2}\left[1 - (exp(-2b_0^2)) \times B_{bsa}\right]\right\}^{\frac{1}{2}} \quad (245)$$

Dimana:

$$B_{bsa} = \begin{cases} 1 + b_0^2 + b_0^4 + \frac{b_0^6}{2} + \frac{b_0^8}{4} + \frac{b_0^{10}}{12} & b_0 \le 1 \\ [exp(2b_0^2)] \times \left[\frac{1}{\sqrt{\pi} b_0}\left(1 - \frac{1}{16 b_0^2}\right)\right] & b_0 > 1 \end{cases} \quad (246)$$

$$b_0 = 0{,}0023 \times \left(\frac{b_e}{T}\right) \quad (247)$$

Keterangan:

b_e adalah ukuran fondasi efektif (dalam m)

$$b_e = \sqrt{A_{base}} \le 80 \text{ m} \quad (248)$$

$200 \le v_s \le 500$ (m/s)

T = periode untuk menghitung respons spektra, yang tidak boleh diambil kurang dari 0,2 detik ketika digunakan pada Persamaan (247)

A_{base} = luas dari dasar struktur (m^2)

Faktor modifikasi untuk penanaman, RRS_e, harus ditentukan menggunakan Persamaan (249) untuk setiap periode yang dibutuhkan dalam analisis.

$$RRS_e = 0{,}25 + 0{,}75 \times cos\left(\frac{2\pi e}{T v_s}\right) \quad (249)$$

Keterangan:

e = kedalaman penanaman fondasi, tidak lebih besar dari 6,1 meter. Sedikitnya 75 % dari tapak fondasi harus mencapai kedalaman penanaman. Fondasi untuk struktur yang berada pada daerah lereng harus diambil dari kedalaman penanaman terkecil

v_s = kecepatan gelombang geser efektif rata-rata pada tanah, diambil sebagai rata-rata dari nilai kecepatan sepanjang kedalaman penanaman dari fondasi yang ditentukan berdasarkan v_{so} dan Tabel 39 atau berdasarkan penyelidikan tanah spesifik situs dan tidak boleh lebih kecil dari 200 m/s

v_{so} = kecepatan gelombang geser rata-rata fondasi pada tingkat regangan kecil sepanjang kedalaman penanaman fondasi

T = periode untuk menghitung nilai respons spektra, tidak boleh diambil lebih kecil dari 0,2 detik apabila digunakan padaPersamaan (249)

Kombinasi ITS Kinematik dan Inersial

- Tidak ada consensus umum
- Paling konservatif, dijumlahkan, namun hal ini dirasakan sangat konservatif

- Gailbraith, Maeem, dan Bruin, "Evaluation of Marine Structures for Kinematic Effects," PIANC-World Congress, Panama, 2018
  - Post Kinematic (static push over)

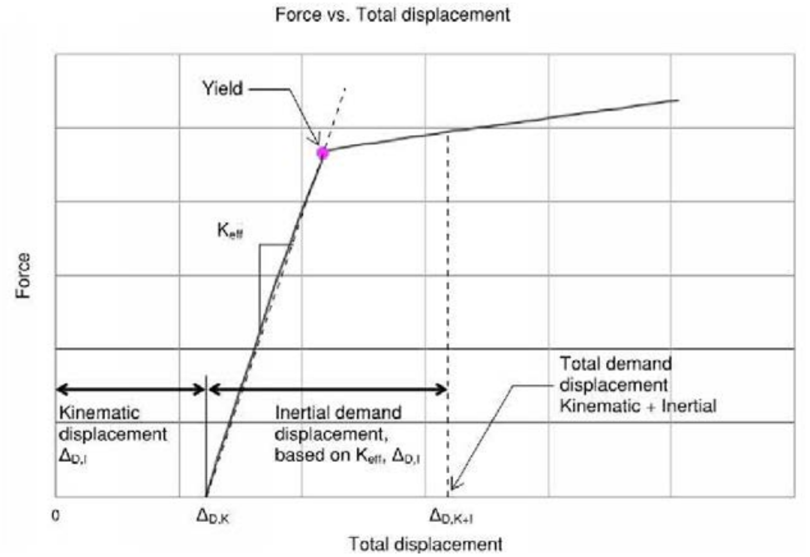

Beban Inersia Gempa pada Basement dan Fondasi Tiang

Provisi Gempa Minimum: (7.8.1.1)

$$E_h = 0.044\ S_{DS}\ I_e\ W_b = 0.044\ 2/3\ F_a\ S_{a,MCER} \geq 0.01$$

Historis (SNI 1726 2002):

$F_b = 0.10\ A_o\ I\ W_b$ di mana $A_o = PGA$ (setara $2/3\ PGA_{MCEG}$ dengan $F_{PGA} \sim F_a$)

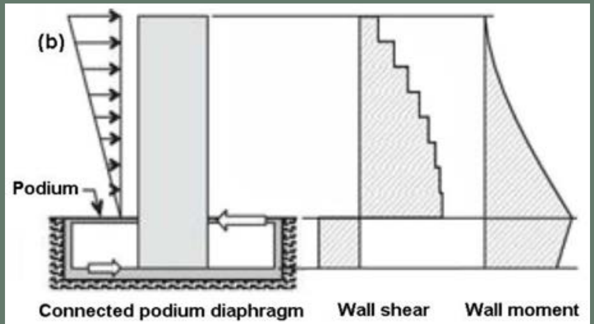

Merujuk Japan's Building Standard Law (2001):

$$F_b = k\ W_b$$

$$\text{di mana } k = \begin{cases} 0.1\ A_0\ \left(1 - \frac{D}{40}\right) \text{for } D \leq 20\text{m} \\ 0.05\ A_0 \text{ for } D > 20\text{ m} \end{cases}$$

$$F_{tiang} = (E_{U\text{-}Str} + \sum k\ W_b)\ (1 - 0.2\ \sqrt{H}\ /\ D_f^{0.25}) \quad \rightarrow 0.2\ \sqrt{H}\ /\ D_f^{0.25} \text{ vs } \frac{1+1.5\ \alpha\ \frac{H}{d}}{\frac{K_{core}}{K_{BS}}}$$

backstay effect

di mana $E_{U\text{-}Str}$ adalah beban gempa struktur atas,

H adalah tinggi total bangunan

D_f adalah kedalaman COL fondasi dari permukaan tanah

Karimi, M., et al., "Relationship for prediction of backstay effect in tall buildings with core-wall system," *Advances in Computational Design, Vol 5. No. 1* (20220)

Building Research Institute, Ministry of Land, Infrastructure and Transport, "*The Technical background of structural requirements in the revised Building Standard Law,*" in Japanese, 2001

Beban Kinematik Gempa pada Basement

Basement: *Base Slab Averaging* (14.4):

$$RRS_{bsa} = 0.25 + 0.75 \quad \left\{\frac{1}{b_0^2}\left[1 - \left(\exp(-2b_0^2)\right)B_{bsa}\right]\right\}^{1/2}$$

$$B_{bsa} = \begin{cases} 1 + \ b_0^2 + b_0^4 + \dfrac{b_0^6}{2} + \dfrac{b_0^8}{4} + \dfrac{b_0^{10}}{12} & b_0 \leq 1 \\ [\exp(2b_0^2)]\left[\dfrac{1}{b_0\sqrt{\pi}}\left(1 - \dfrac{1}{16b_0^2}\right)\right] & b_0 > 1 \end{cases}$$

$$b_0 = 0.0023\left(\frac{\sqrt{A_{base}}}{T}\right) \qquad \text{di mana } \sqrt{A_{base}} \leq 80 \text{ m}$$

and

$$RRS_e = 0.25 + 0.75 \cos\left(\frac{2\pi e}{Tv_s}\right) \qquad \text{di mana } e = \text{embedment depth, dan T} > 0.2 \text{ detik}$$

Beban kinematic pada basement??

Beben Kinematik Gempa pada Fondasi Tiang

Modifikasi Respon Spektra:

- (Turner, B.J., Brandenberg, S.J., Stewart, J.P., Influence of Kinematic SSI on Foundation Input Motions for Bridges on Deep Foundations, Pacific Earthquake Engineering Research Center, Univ. California, Berkeley, PEER Report No. 2017/08, November 2017).

Tiang: ASCE 7-16 14.2.3:

- Persyaratan tulangan fondasi tiang beton (panjang tulangan memanjang dan transverse, terkait dengan perbedaan kekakuan antar lapisan, momen retak tiang beton dsb).

Kinematic Tiang

Fungsi Transfer Respon Spektra Percepatan,

PSA_{FIM} = Percepatan Puncak Spektra *FIM*

PSA_{FFM} = Percepatan Puncak Spektra *FF*

B = diameter of pile

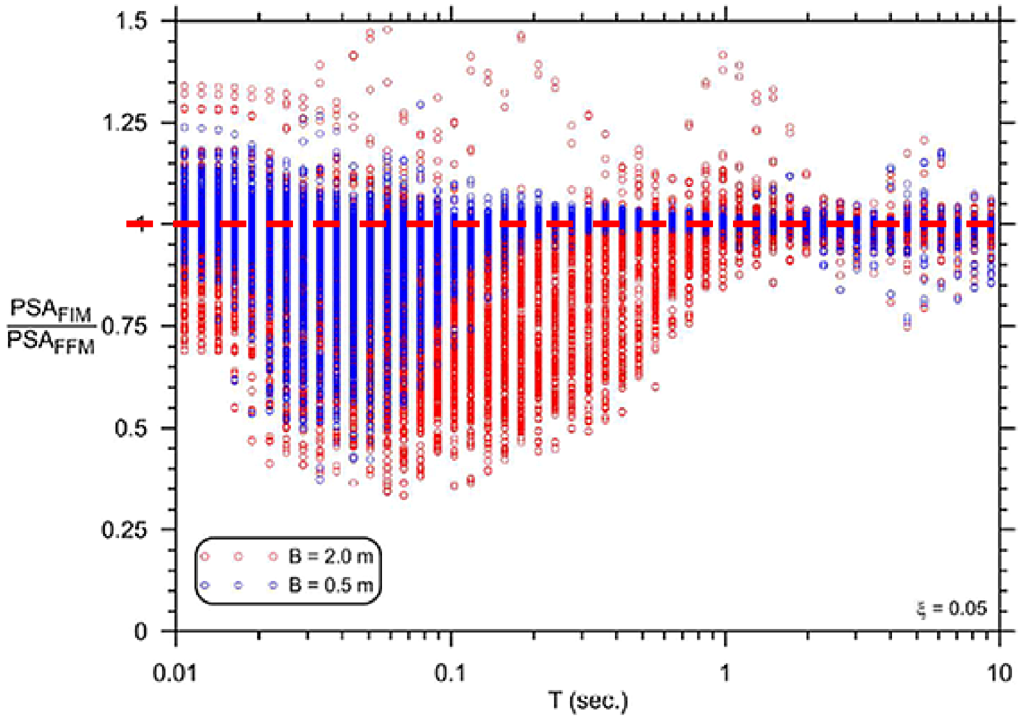

Figure 4.35 Fixed-head spectral ratio results.

Turner, B. J., Brandenberg, S. J., Stewart, J. P., 2017, "Influence of Kinematic SSI on Foundation Input Motions for Bridges on Deep Foundations," Pacific Earthquake Engineering Research Center, PEER Report No. 2017/08.

SNI 1726-2019

ASCE 7-16 Section 14.2.3:

7.13.7 Persyaratan untuk struktur yang didesain untuk kategori desain seismik D sampai F

Sebagai tambahan pada persyaratan 6.7.2, 6.7.3 dan persyaratan desain lainnya, persyaratan desain fondasi berikut harus diterapkan pada struktur yang didesain untuk kategori desain seismik D, E, atau F. Desain dan konstruksi komponen fondasi beton harus memenuhi persyaratan di SNI 2847, kecuali seperti dimodifikasi oleh persyaratan pasal ini.

PENGECUALIAN Hunian satu dan dua keluarga terpisah dari konstruksi rangka ringan dengan tinggi tidak melebihi dua tingkat di atas tanah hanya perlu sesuai dengan persyaratan untuk 6.7.2, 6.7.3 (Butir 2 sampai 4) 7.13.2, dan 7.13.6.

7.13.8.3.3 Detail fondasi tiang beton

Fondasi tiang beton termasuk fondasi tiang bor dan tiang pracetak harus didetailkan sesuai dengan Pasal 18.7.5 pada SNI 2487 yang berlaku dari bagian atas tiang hingga kedalaman terdalam tanah terlikuifaksi ditambah sedikitnya 7 kali dimensi penampangan elemen fondasi.

14.2.3.2 Concrete Pile Requirements for Seismic Design Categories D through F. Concrete piles in structures assigned to Seismic Design Category D, E, or F shall comply with Section 14.2.3.1.1 and the requirements of this section.

14.2.3.2.1 Site Class E or F Soil. Where concrete piles are used in Site Class E or F, they shall have transverse reinforcement in accordance with Sections 18.7.5.2 through 18.7.5.4 of ACI 318 within seven pile diameters of the pile cap and of the interfaces between strata that are hard or stiff and strata that are liquefiable or are composed of soft to medium stiff clay.

ASCE 7-16 Section 14.2.3:

14.2.3.2.3 Reinforcement for Uncased Concrete Piles (SDC D through F). Reinforcement shall be provided where required by analysis. For uncased cast-in-place drilled or augered concrete piles, a minimum of four longitudinal bars with a minimum longitudinal reinforcement ratio of 0.005 and transverse confinement reinforcement in accordance with ACI 318, Sections 18.7.5.2 through 18.7.5.4 shall be provided throughout the minimum reinforced length of the pile as defined below starting at the top of the pile. The longitudinal reinforcement shall extend beyond the minimum reinforced length of the pile by the tension development length.

The minimum reinforced length of the pile shall be taken as the greatest of

1. One-half of the pile length;
2. A distance of 10 ft (3 m);
3. Three times the pile diameter; or
4. The flexural length of the pile, which shall be taken as the length from the bottom of the pile cap to a point where the concrete section cracking moment multiplied by a resistance factor of 0.4 exceeds the required factored moment at that point.

In addition, for piles located in Site Classes E or F, longitudinal reinforcement and transverse confinement reinforcement, as described above, shall extend the full length of the pile.

Kinematic Tiang

<u>Fungsi Transfer Kinematik</u>,

$H_u = |u_p| / |u_g|$

u_p = deformasi lateral tiang di muka tanah

u_g = deformasi muka tanah *FF*

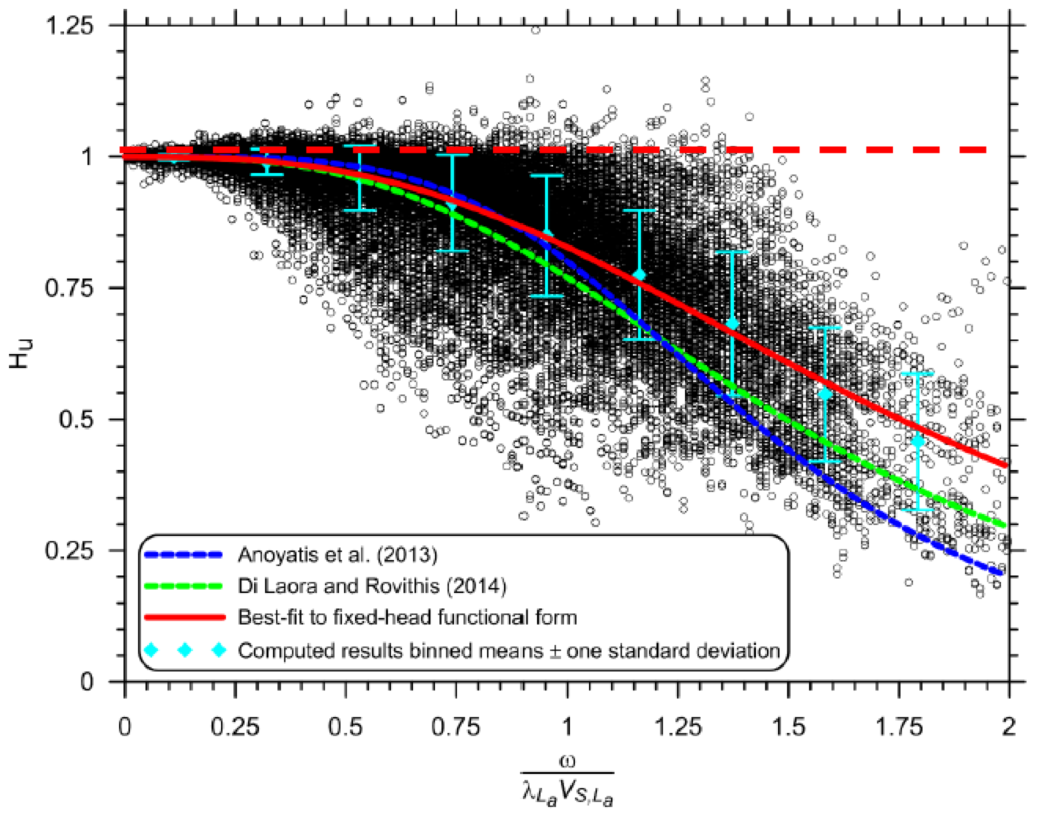

Figure 4.13 Normalized horizontal displacement transfer function results for fixed-head piles.

Kinematic Tiang

<u>Fungsi Transfer Kinematik</u>,

$H_u = |u_p| / |u_g|$

u_p = deformasi lateral tiang di muka tanah

u_g = deformasi muka tanah *FF*

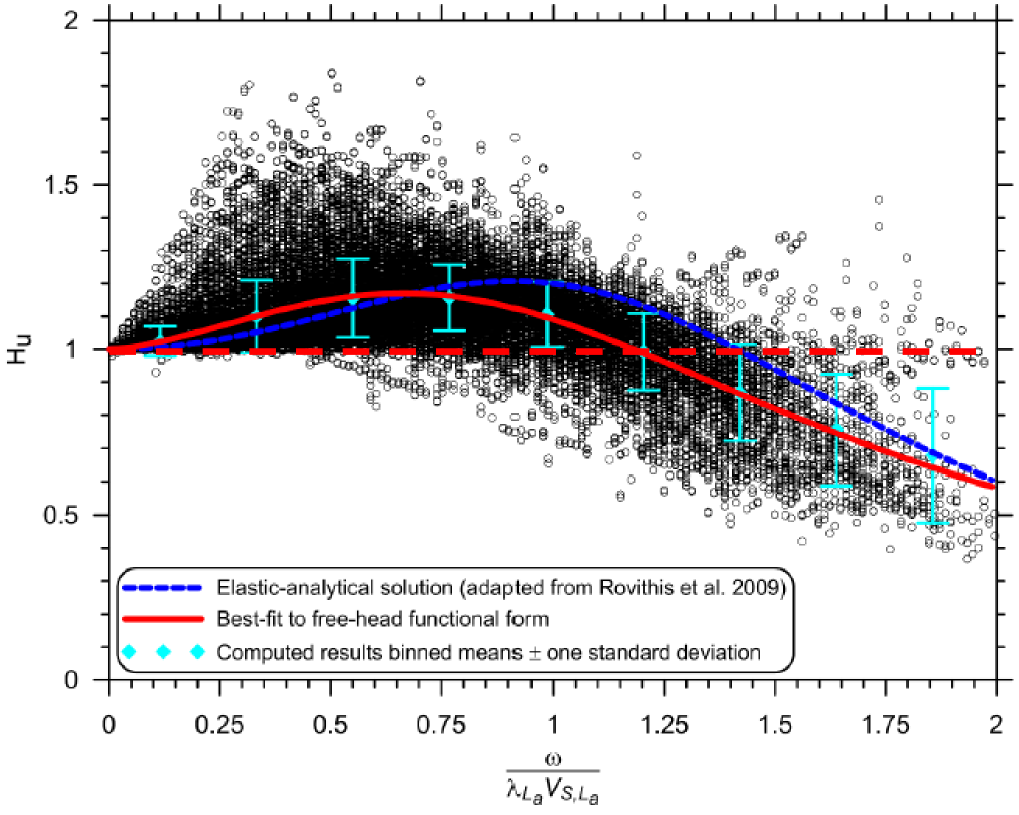

Figure 4.14 **Normalized horizontal displacement transfer function results for free-head piles.**

Kinematic Tiang

Fungsi Transfer Kinematik,

$H_\theta = |\theta_p| / |\theta_g|$

θ_p = rotasi tiang di muka tanah

θ_g = rotasi muka tanah *FF*

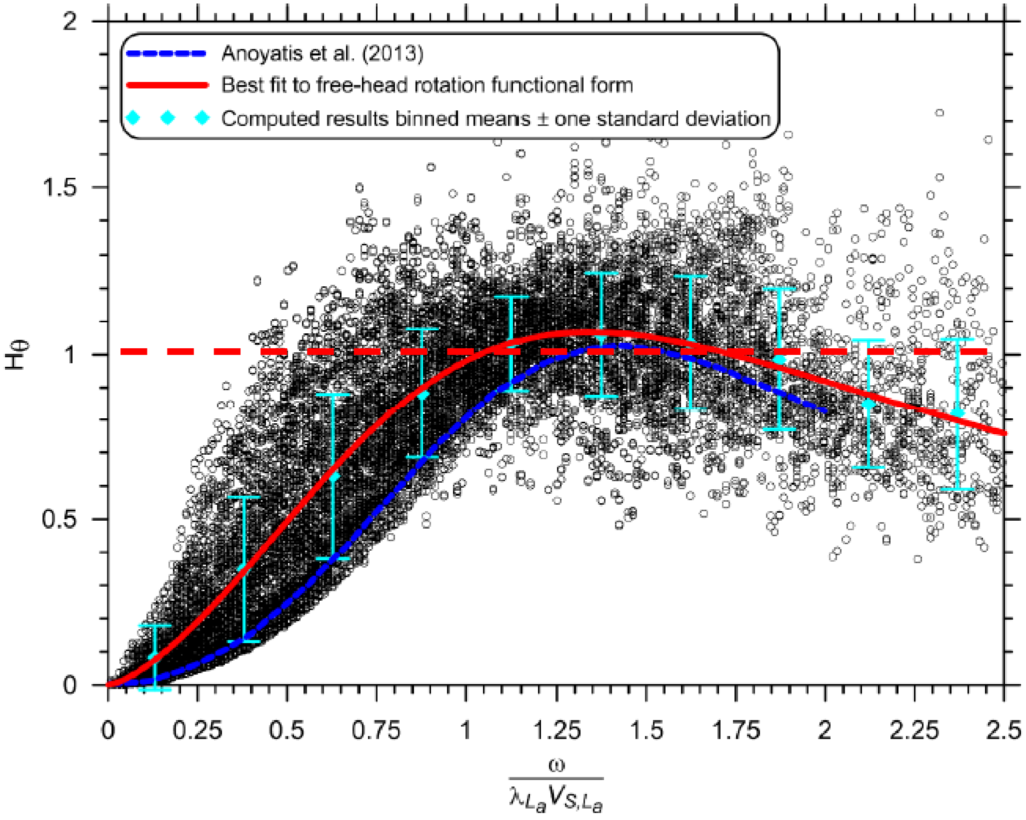

Figure 4.15 **Normalized rotation transfer function results for free-head piles.**

Tekanan lateral gempa pada dinding

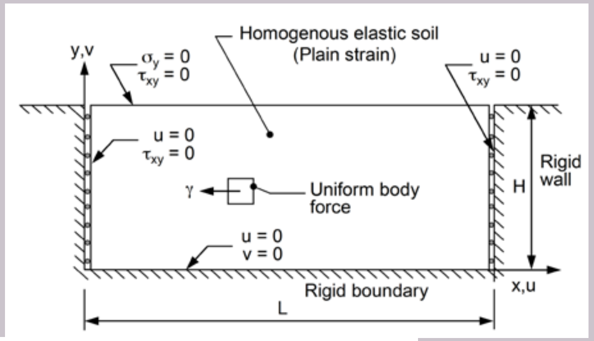

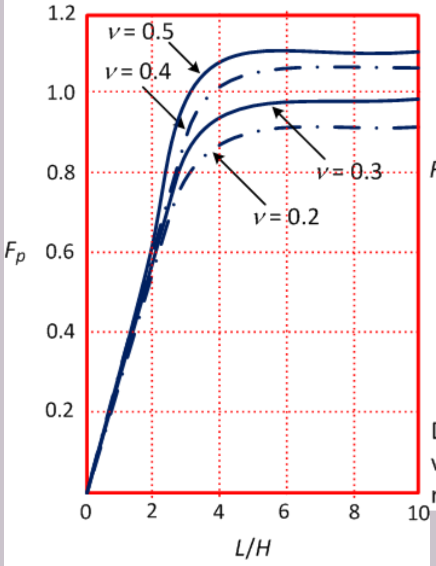

Dimensionless thrust factor for various geometries and soil Poisson's ratio values. After Wood (1973).

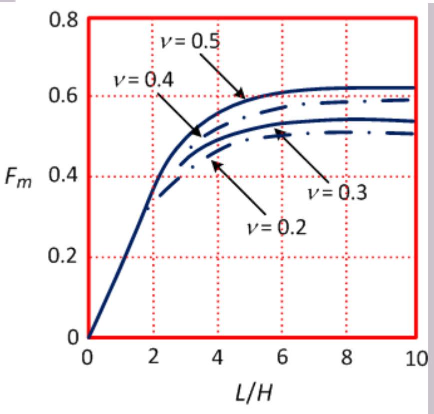

Dimensionless moment factor for various geometries and soil Poisson's ratio values. After Wood (1973).

<u>Wood (1973):</u>

$$\Delta P_{eq} = \gamma H^2 \frac{a_h}{g} F_\rho$$

$$\Delta M_{eq} = \gamma H^3 \frac{a_h}{g} F_m$$

$$h_{eq} = \frac{\Delta M_{eq}}{\Delta P_{eq}}$$

Wood, J. H. (1973), *Earthquake induced soil pressures on structures*, PhD Thesis, California Institute of Technology, Pasadena, CA.

Tekanan lateral gempa pada dinding

Others:

- Steedman, R. S., dan Zeng, X., (1990), “The seismic response of waterfront retaining walls,” *Proceedings, ASCE Specialty Conference on Design and Performance of Earth Retaining Structures, STP Publication 25*, Cornell Univ., Ithaca, NY.
- Wu, G., dan Finn, W. D. L., (1996), “Seismic Pressures against Rigid Walls,” *ASCE STP No. 80.*
- Mylonakis, G., Kloukinas, P., dan Papatonopoulos, C., (2007), “An alternative to the Mononobe-Okabe Equation for Seismic Earth Pressures,” *Soil Dynamics and Earthquake Engineering*, (27) 10.

Tekanan Fluida di luar Dinding

(Outboard Fluid Pressure)

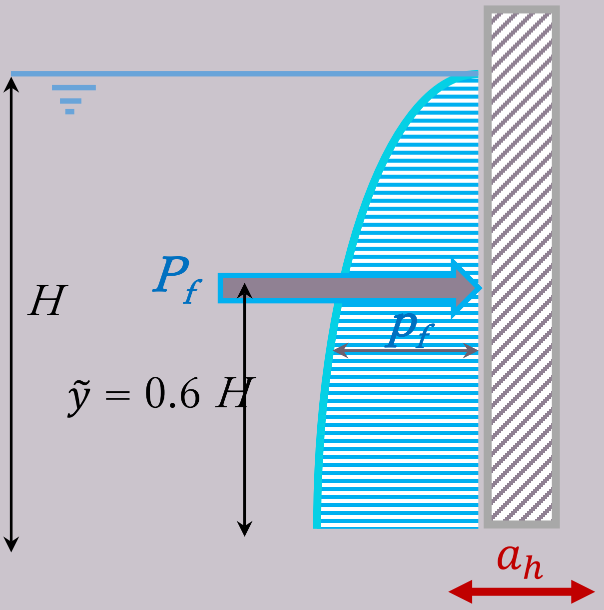

<u>Westergaard (1931)</u>

- $p_f = \frac{7}{8}\frac{\boldsymbol{a_h}}{g}\gamma_f\sqrt{(z_f H)}$
- $P_f = \frac{7}{12}\frac{a_h}{g}\gamma_f H^2$
- $\tilde{y} = 0.6\ H$

<u>Chwang and Housner (1977):</u>

Momentum,
Hydrodynamic Flow:

- $p = C_p\ \rho\ \boldsymbol{a_o}\ h$

Percepatan dinding

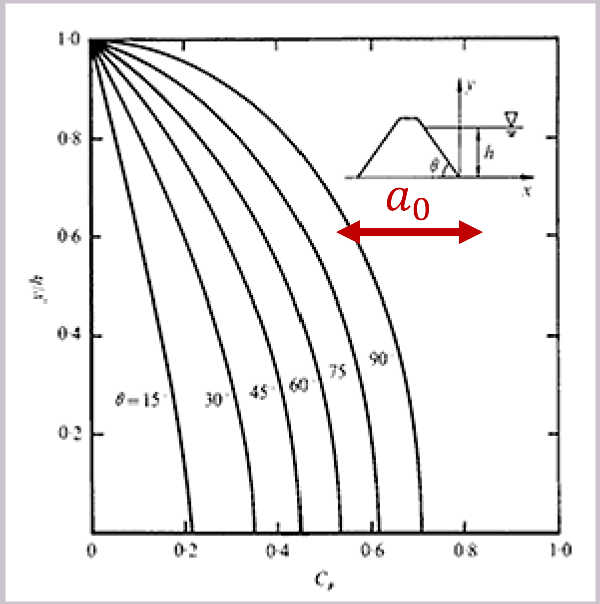

Westergaaard, H.M., (1931), "Water Pressures on Dams during Earthquakes," *ASCE Transactions*, Nov. 1931.
Chwang, A. T., dan Housner, G., (1977), "Hydrodynamic Pressures on Sloping Dams during Earthquakes," Part 1 – Momentum Methods, *Journal of Fluid Mechanics, Vol. 87 Part 2.*

Uji Model Sherif & Fang (1984)

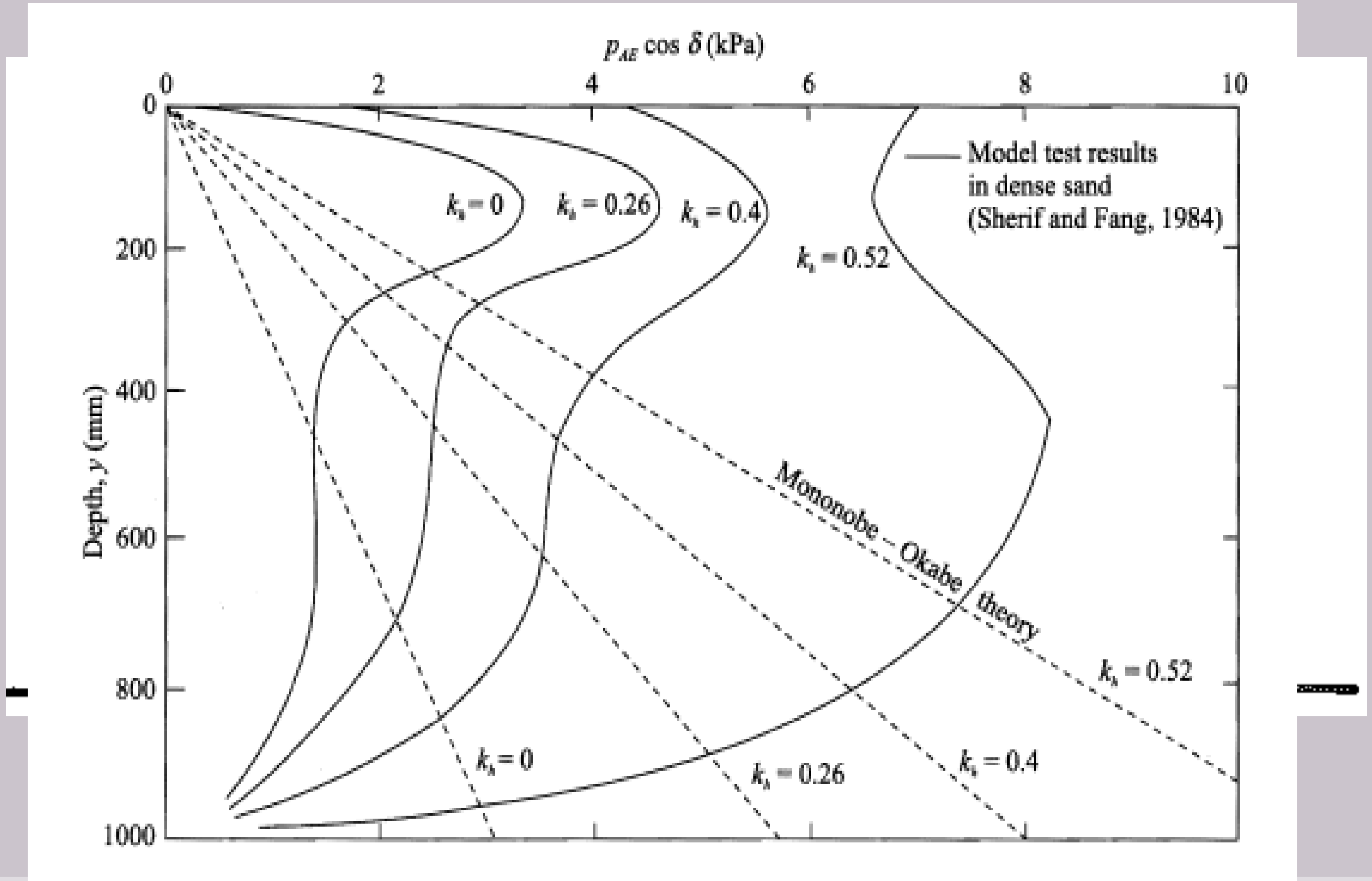

Uji Centrifugal Nakamura (2006)

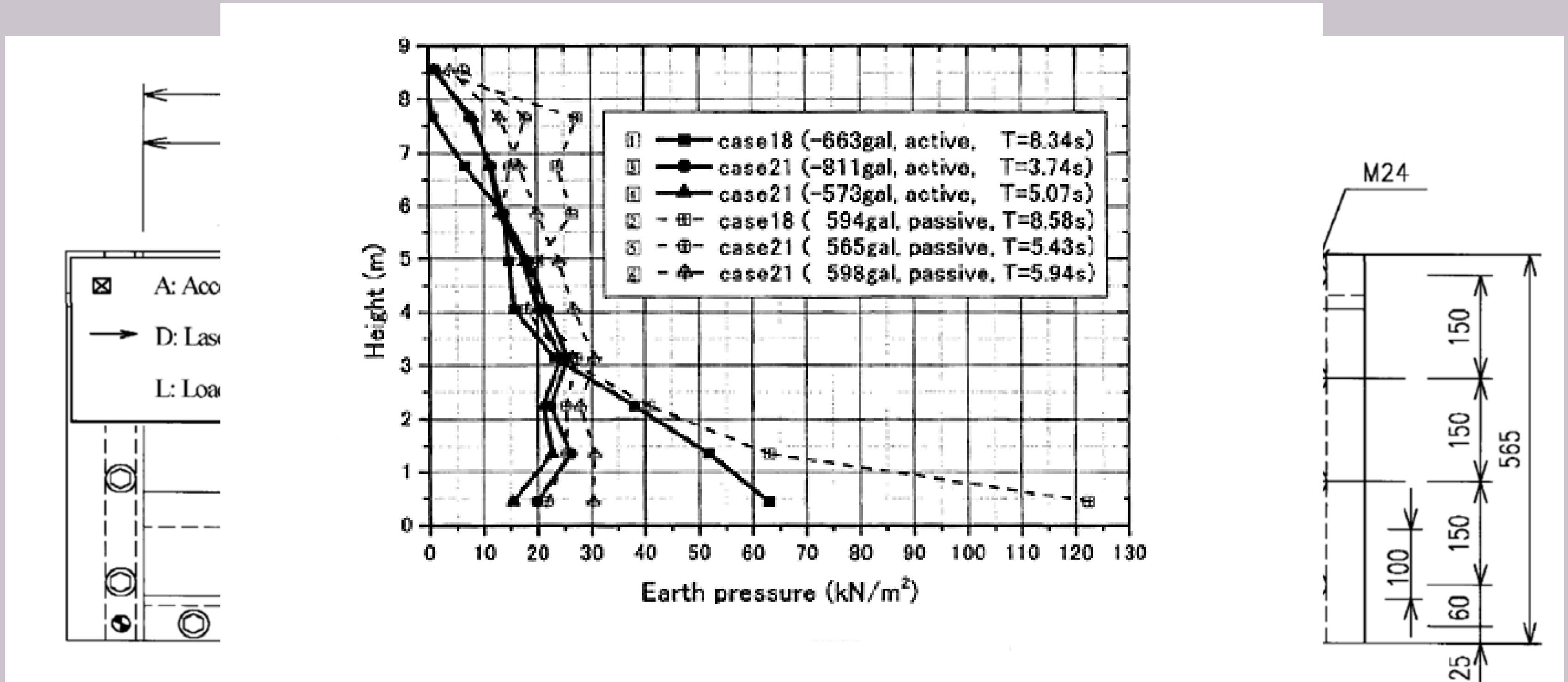

Nakamura, S. 2006. Reexamination of Mononobe-Okabe Theory of Gravity Retaining Walls Using Centrifuge Model Tests, Soils and Foundations, Vol. 46, No.2, 135-146.

Uji Centrifugal Mikola dan Sitar (2013)

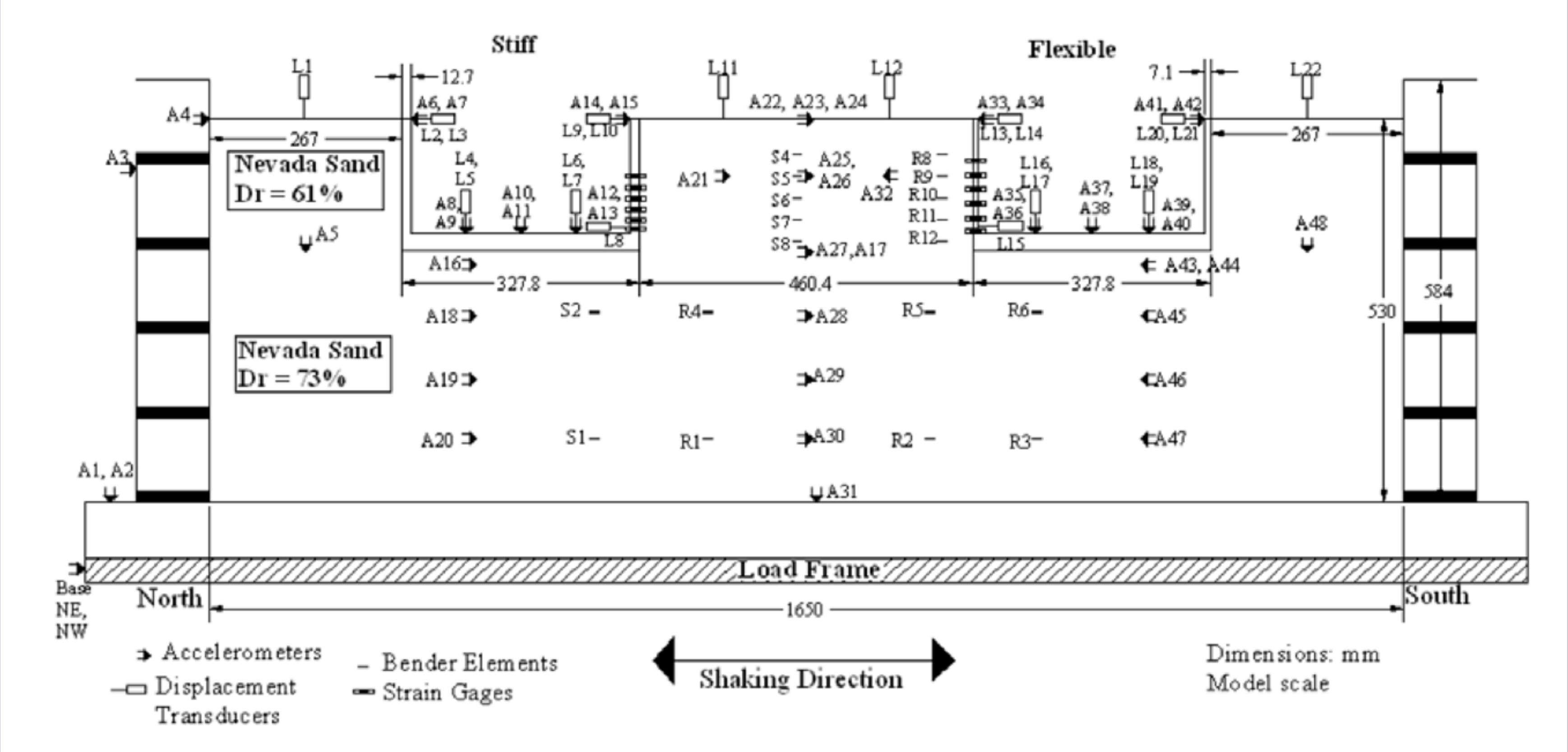

Mikola, R. G., dan Sitar, N., 2013, "Seismic Earth Pressures on Retaining Structures in Cohesionless Soils," Univ. of California Berkeley, Report No. UCB GT 13-01

Uji Centrifugal Mikola dan Sitar (2013)

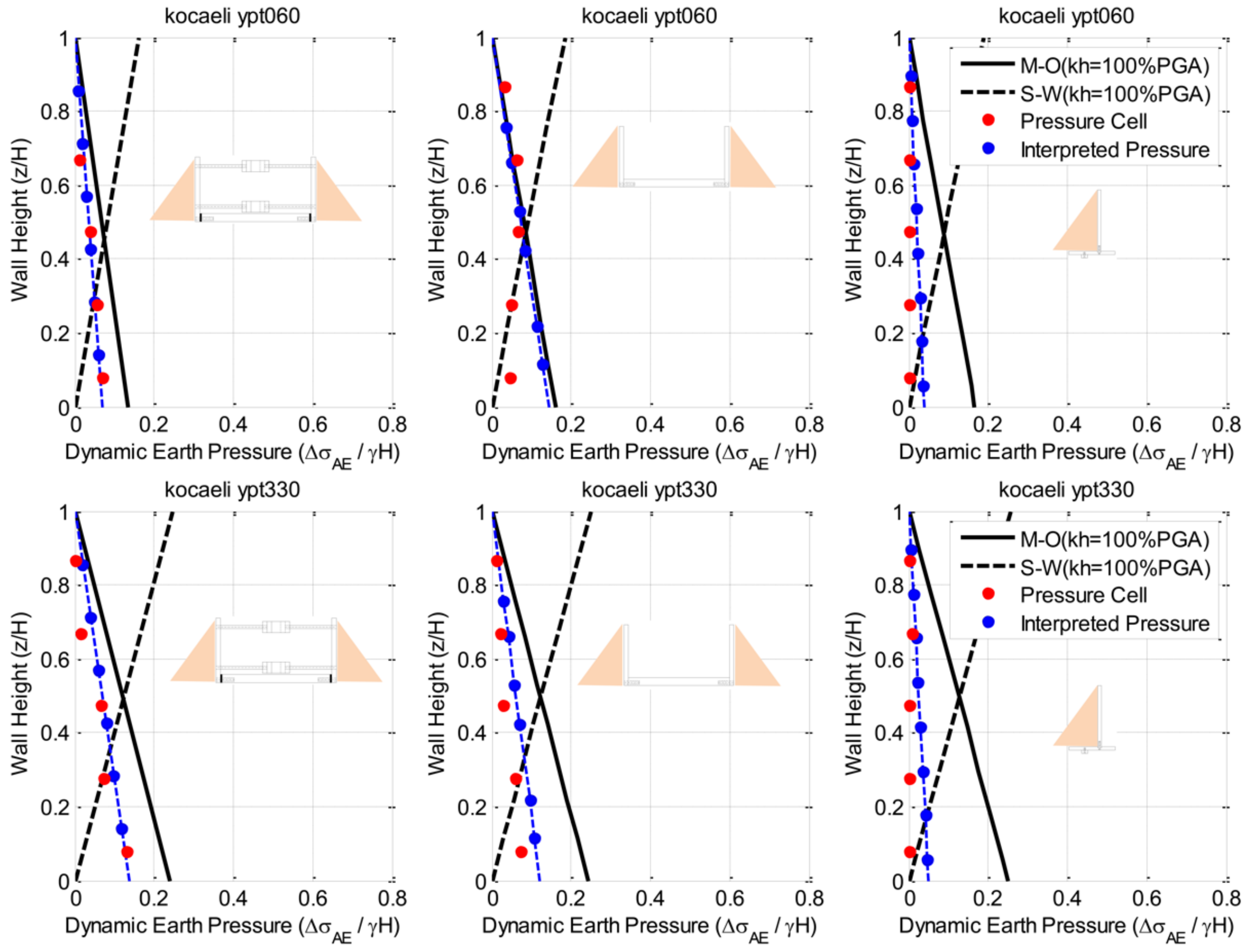

Figure 4.25. Dynamic earth pressure distributions directly measured and interpreted from the pressure sensors and strain gage and load cell data and estimated M-O as well as S-W on walls for Kocaeli-YPT060-3 (PGA_{ff}=0.25), Kocaeli-YPT330-2 (PGA_{ff}=0.34).

Uji Centrifugal Mikola dan Sitar (2013)

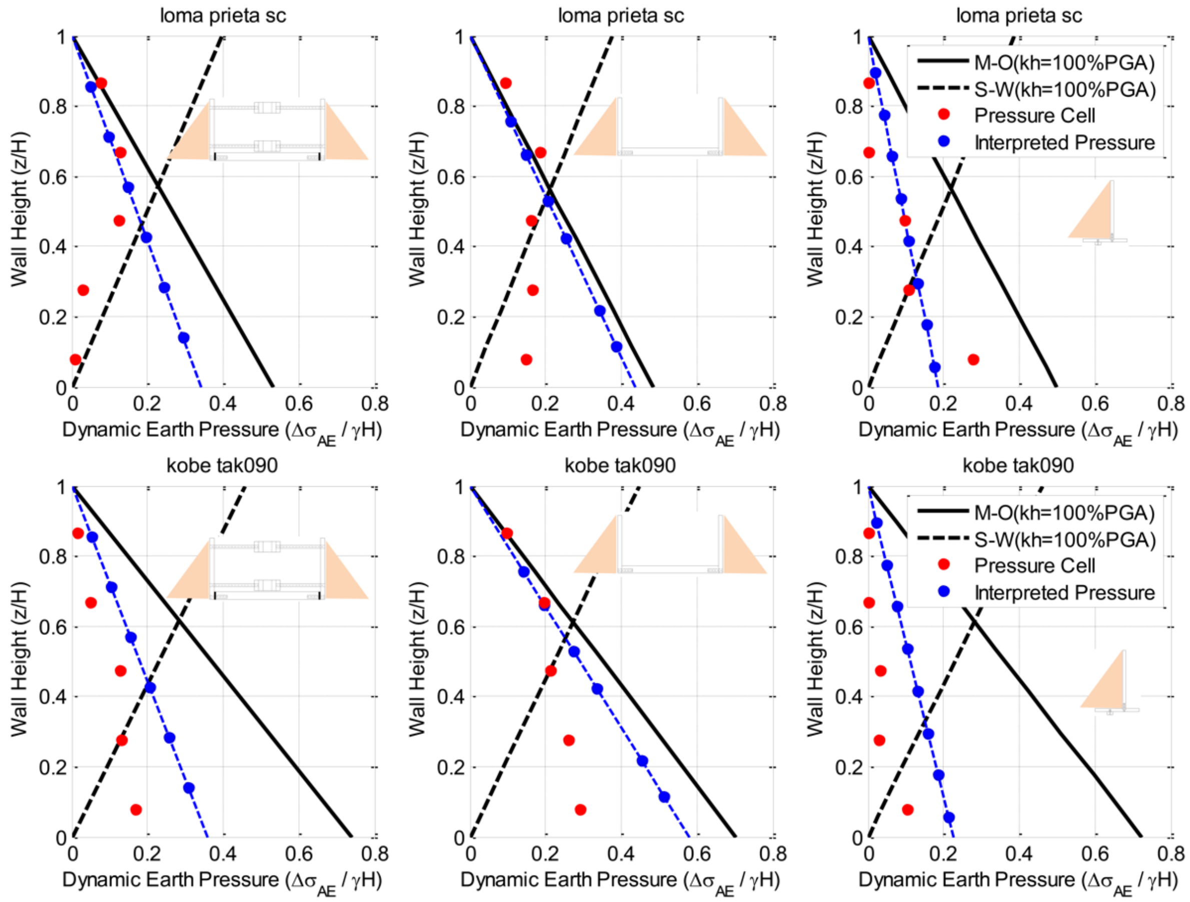

Figure 4.26. Dynamic earth pressure distributions directly measured and interpreted from the pressure sensors and strain gage and load cell data and estimated M-O as well as S-W on walls for Loma Prieta-SC-1 (PGA_{ff}=0.51), Kobe-TAK090-2 (PGA_{ff}=0.61).

Uji Centrifugal Mikola dan Sitar (2013)

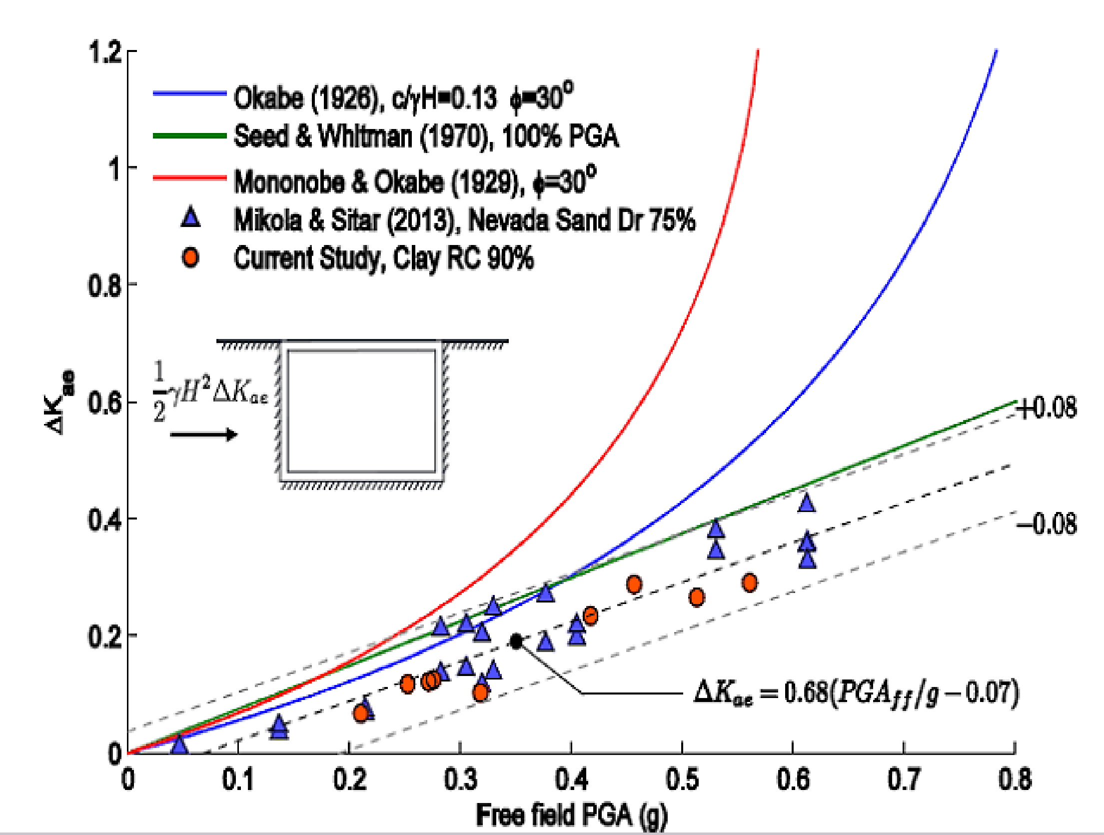

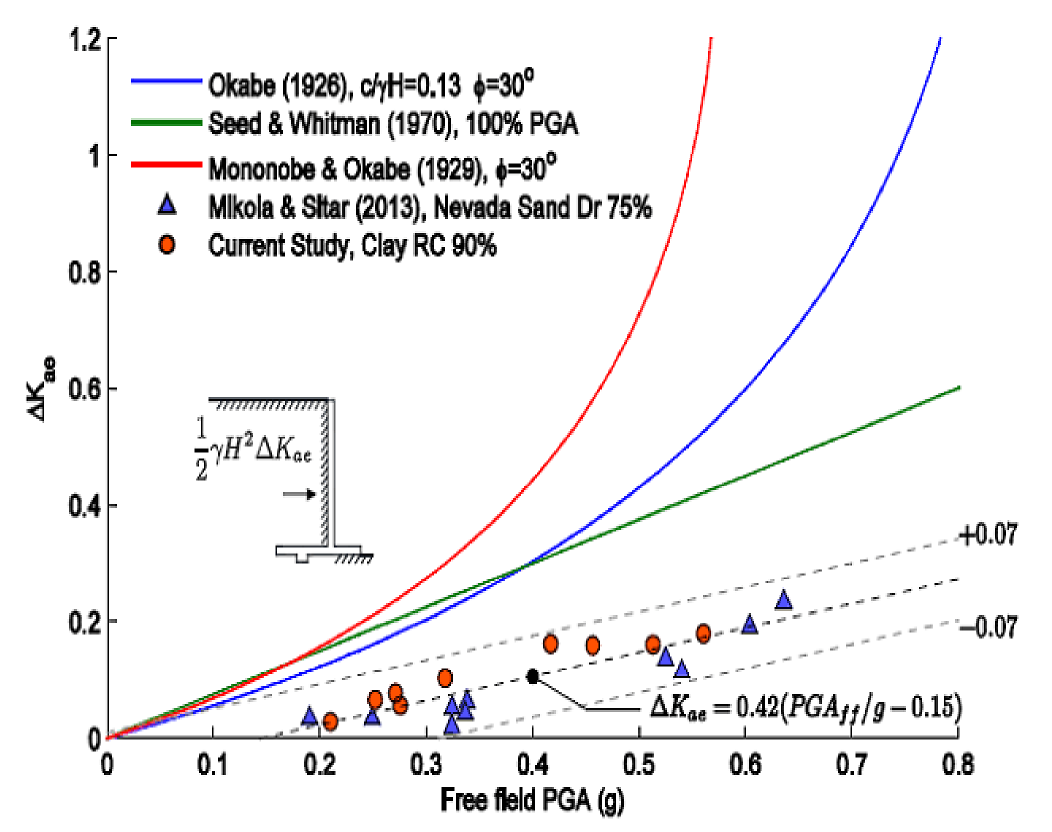

Mikola, R. G., dan Sitar, N., 2013, “Seismic Earth Pressures on Retaining Structures in Cohesionless Soils,” Univ. of California Berkeley, Report No. UCB GT 13-01

Marshall Lew, et al., “Seismic Earth Pressures on Deep Building Basements,” *SEAOC 2010 Convention Proceedings*

- Untuk tanah tak jenuh, cukup gunakan tekanan lateral K_o (dengan faktor beban 1.6), dan abaikan tekanan seismic.
- Bilamana tekanan aktif statik disertakan, gunakan $k_h \approx 60$ % PGA dan gunakan faktor beban =1.0 (bukan 1.6) untuk komponen seismik.

Conclusions and Summary

When considering the load conditions given in IBC, it appears that building basement walls analyzed and designed using at rest pressures in accordance with the load combination in Eq. (7) may be adequate for seismic earth pressure loading without further analysis. The reason is the different types of earth pressures that must be considered for static versus seismic conditions. As noted above for the seismic load condition represented by Eq. (8), the active earth pressure combined with the seismic increment of earth pressure needs to be considered. Active earth pressures are typically much smaller than at-rest pressures which are commonly on the order of 1.6 to 2.0 times more. Thus as basement walls are conservatively designed for at-rest static pressures using loading combination in Eq. (7) it is very likely that the loading combination in Eq. (8) which is based on active pressures will be automatically satisfied unless the seismic increment of earth pressure is unusually large. With recent research (reported above) indicating that the seismic earth pressures are not as great as indicated by current practice, it would appear that building basement walls retaining level unsaturated earth materials may be considered adequate when just designed for at-rest earth pressures as stipulated in the IBC. Consequently, the current requirement in the seismic provisions to consider seismic earth pressures for such walls may be unnecessary. In retaining walls designed with active pressures, the addition of the seismic increment of soil using loading combination Eq. (8) should still be a consideration and will likely dictate the design of the wall, However, when applying Eq. (8) in this condition, it is recommended that a reduced load factor of 1.0 be used for the seismic increment component of soil in combination with a 1.6 load factor applied to the active pressure component These load factors will more appropriately represent the transitory nature of seismic loading and the low likelihood of load maxima occurring at the same time. To facilitate such loading combinations, the geotechnical engineers would have to separate earth pressure components attributable to the active earth pressure condition and the seismic increment of earth pressure when using the Mononobe-Okabe method.

Taiebat, M., Amirzehni, E., and Finn, W.D.L.," Seismic design of basement walls: evaluation of current practice in British Columbia," *Canadian Geotechnical Journal*, Vol. 51, 2014

1. Paling berbahaya pada basement paling atas, terutama bila ukuran basement atas lebih besar strukturnya lebih sedikit kekanganannya dari bagian di bawahnya.
2. Tipikal k_h = 0.5 to 0.6 PGA sudah memadai untuk kejadian gempa dengan keterlampauan 2% dalam 50 years.
3. MO + Seed & Whitman biasanya OK.

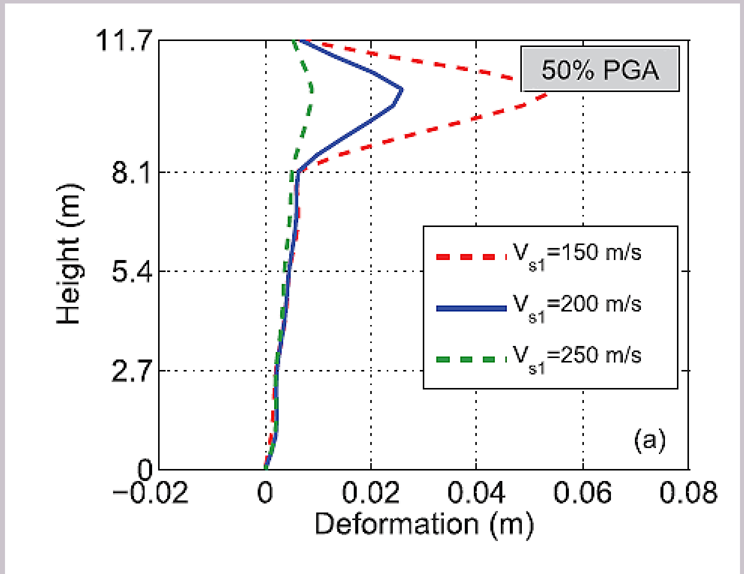

Tokimatsu, et al., “Effects of Inertial and Kinematic Forces on Pile Stresses in Large Shaking Table Tests,” *13th World Conference on Earthquake Engineering*, Vancouver, Canada, 2004

- Bila $T_s < T_g$, gaya gempa inersial dan kinematic bekerja bersamaan.
- Bila $T_s > T_g$, gaya gempa inersial dan kinematic akan berbeda fase, sehingga cukup ditinjau penagruh maximum dari salah satunya.
- Tekanan tanah pada tanah kering biasanya berlawanan dengan gaya inersia; sedangkan untuk tanah jenuh terlikuifaksi, tekanannya akan bekerja bersama dengan gaya inersia.

- If the natural period of the structure is less than that of the ground, the kinematic force tends to be in phase with the inertial force, increasing the stress in piles. The maximum pile stress tends to occur when both inertial force and ground displacement take maxima and act in the same direction.
- If the natural period of the structure is greater than that of the ground, the kinematic force tends to be out of phase with the inertial force, restraining the pile stress from increasing. The maximum pile stress tends to occur when either inertial force or ground displacement take maxima with the other being very small or when both inertial force and ground displacement do not become maxima at the same time.
- The earth pressure in dry sand tends to act against the inertial force, while that in saturated liquefied sand tends to act with the inertial force. This is because the ground displacement becomes large with the development of liquefaction.

Murono, Y, and Nishimura, A., "Evaluation of Seismic Force of Pile Foundation Induced by Inertial and Kinematic Interaction," *12th World Conference on Earthquake Engineering*, Auckland, New Zealand, 2000

- **Tiang linier**, bila $T_s < T_g$, gaya gempa inersial dan kinematic bekerja bersamaan. Bila $T_s > T_g$, gaya gempa inersial dan kinematic akan berbeda jauh fasenya.
- **Tiang non-linier (terjadi sendi plastis di kontras antar lapisan),** gaya gempa inersial dan kinematic bekerja bersamaan, karena gelombang percepatan mempunyai bentuk yang landai.

- For the linear pier model: The seismic response of soil-pile-structure system is much dependent on the relationship between the period of structure T_s and soil deposit T_g. If $T_s < T_g$, the inertia and the kinematic loading will act on the pile with nearly the same phase, while $T_s > T_g$, the delay in phase between them will be very large.
- For the non-linear pier model: Though inertial force itself is reduced due to the pier yielding, the possibility becomes high that the soil displacement and the inertial force take maximum values simultaneously, because the acceleration wave pattern has a flat shape.

Pengaruh lereng tanah pada beban seismik basemen dan fondasi

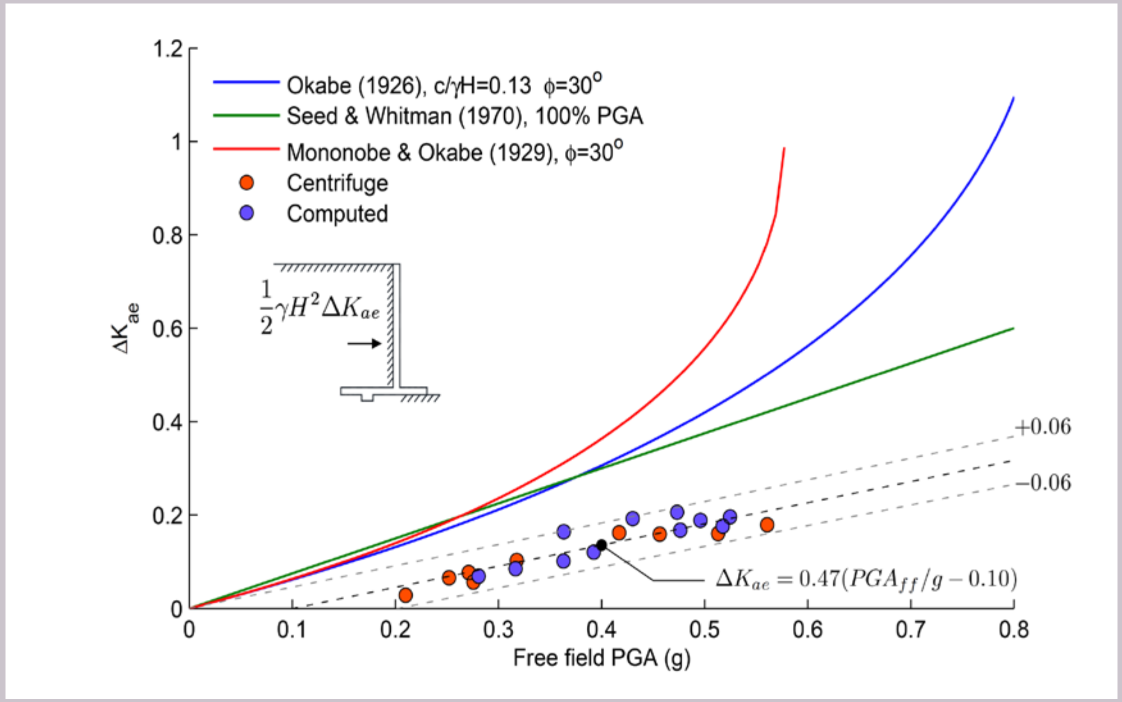

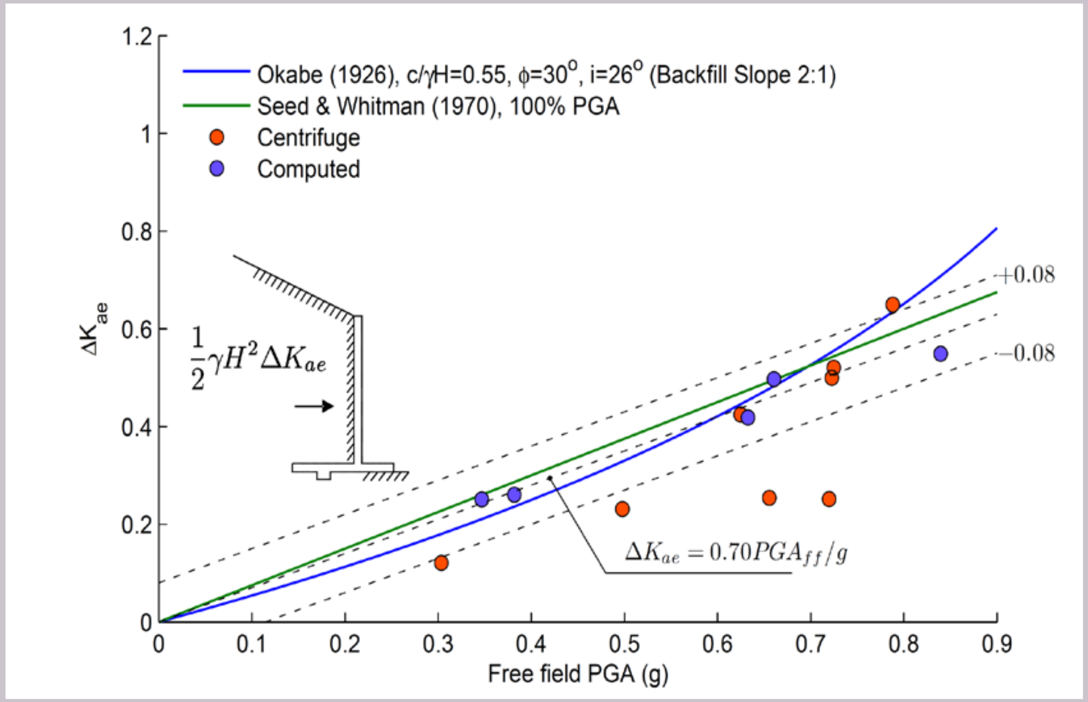

Agusti, G. C., dan Sitar, N., (2013), “Seismic Earth Pressures on Retaining Structures in Cohesive Soils,” Univ. of California, Berkeley, Report No. UCB GT 13-02

Pengaruh lereng tanah pada beban seismik basemen dan fondasi

Comparison of K_{0E} for horizontal & 27º (2H:1V) sloped backfills (ϕ=32º and 40º)

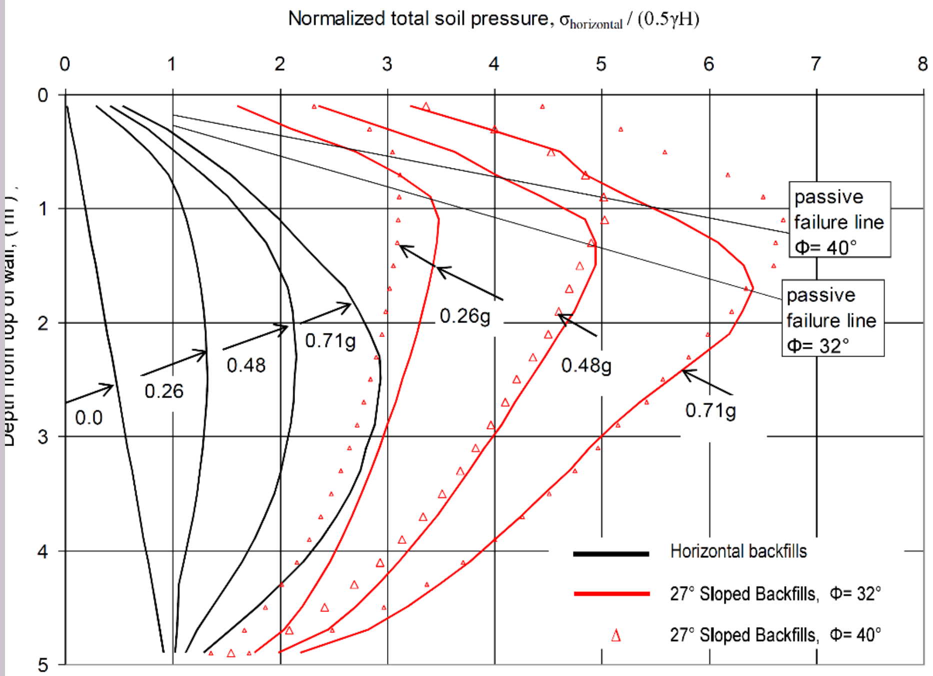

$P_{0E} = \frac{1}{2} K_{0E}\, \gamma H^2$

K_{0E} is a soil pressure coefficient, proposed for rigid wall (*new*)

A_{max}	Hori. ϕ=32º	2H:1V ϕ=32º	2H:1V ϕ=40º
0.0g	0.47	1.5	1.1
0.26g	1.1	2.8	2.6
0.48g	1.7	3.8	3.8
0.71g	2.2	4.8	5.0

Wu, G., (2010), "Seismic lateral pressures for design of rigid walls," *Proc. 5th International Conference on Recent Advances in Geotechnical Earthquake Engineering and Soil Dynamics,* San Diego, Ca.

Pengaruh likuifaksi pada basement dan fondasi

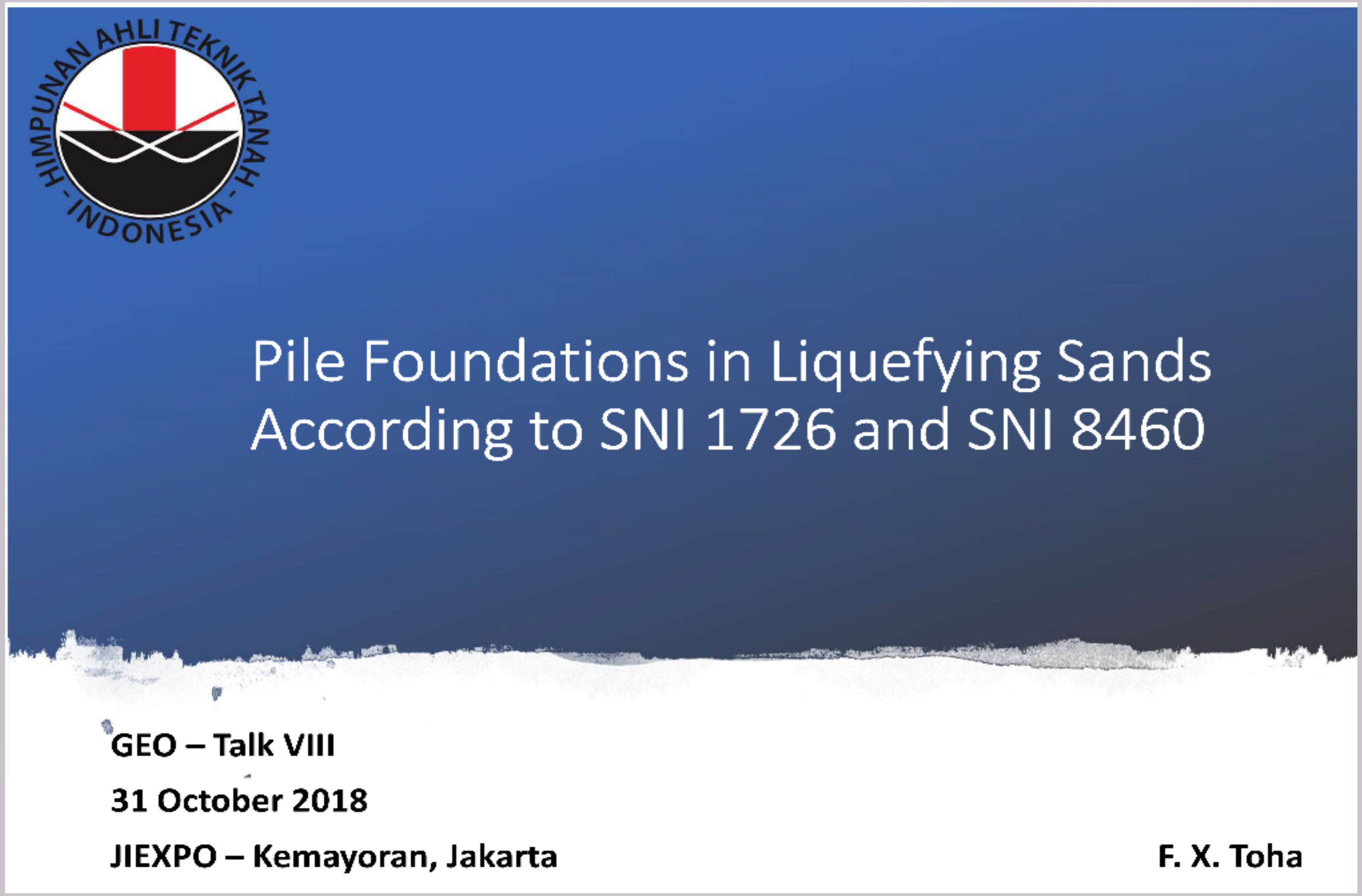

SNI 1726 2019 dan AASHTO 2017

Analisis dilakukan dalam kondisi *liquefied* dan *non-liquefied* (**7.13.8,** ASCE 7-16 12.13.9, AASHTO 2017).

Kasus 1. Spektra tanpa likuifaksi, 100 % gaya inersial dan kinematik (tanpa sebaran lateral).

Kasus 2. Tanah terlikuifaksi, 100% kinematic (dengan sebaran lateral) + 50% inersial.

Kasus 3. Tanpa likuifaksi, menggunakan *plastic demand* struktur atas.

Kasus 4. Dengan likuifaksi, menggunakan *plastic demand* struktur atas.

p-y curve for liquefied sand (residual strength approach)

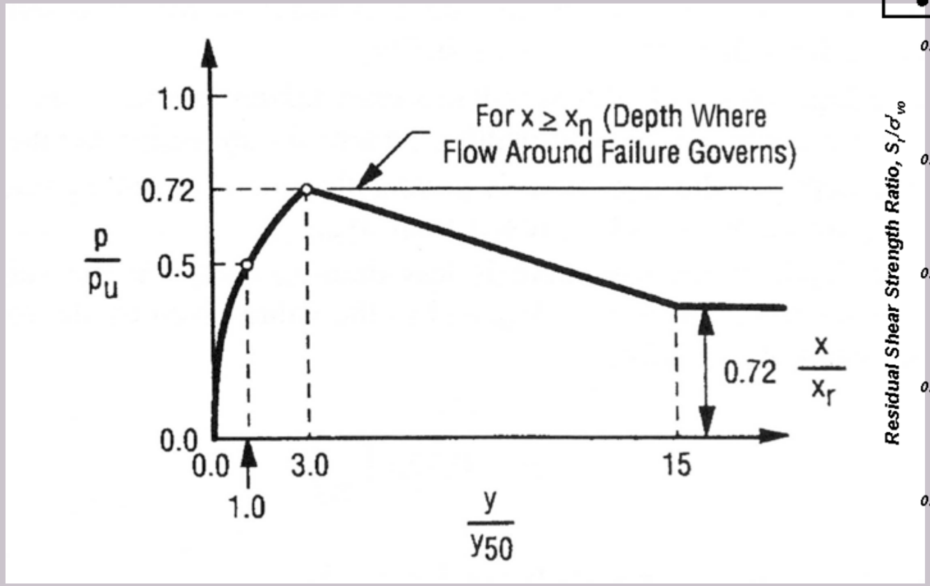

p-y curve for liquefied sand
(=soft clay, saturated, cyclic load)

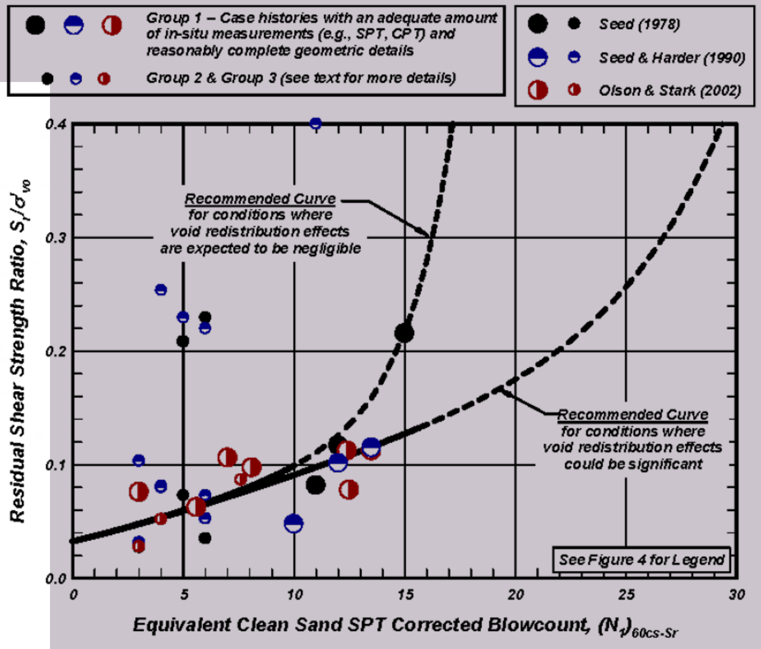

Fines Content, FC (% passing No. 200 sieve)	$\Delta(N_1)_{60\text{-}Sr}$
10	1
25	2
50	4
75	5

p-y curve for liquefied sand (degradation factor approach)

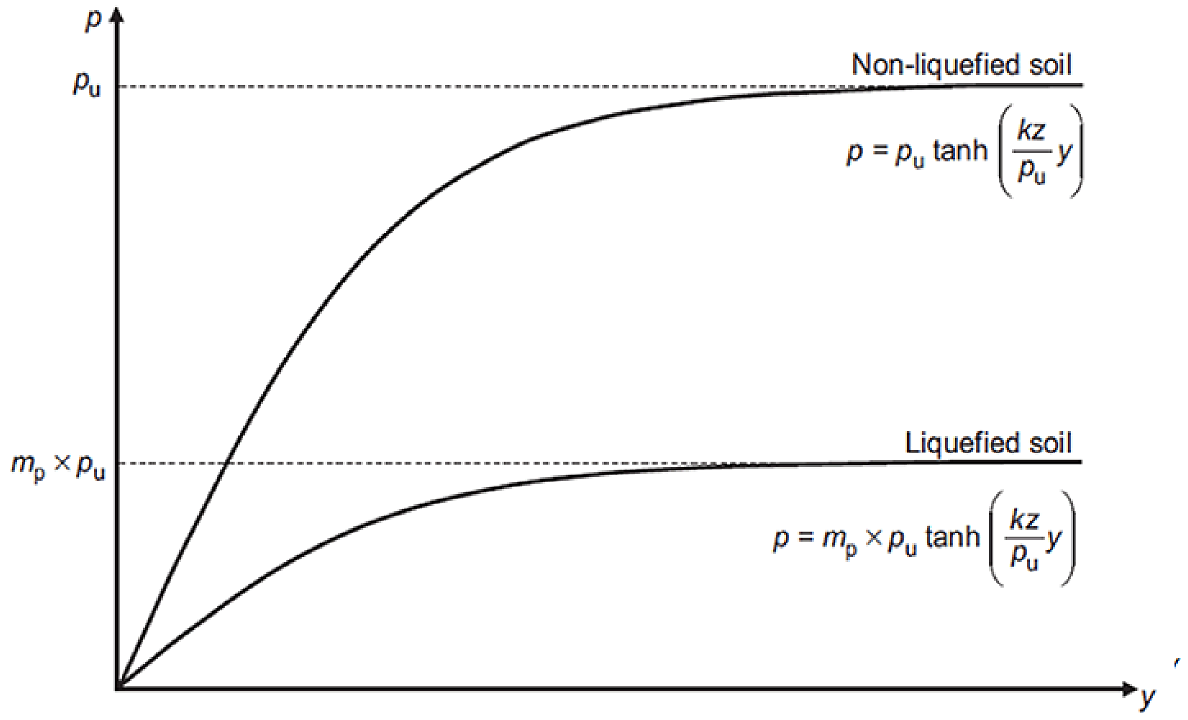

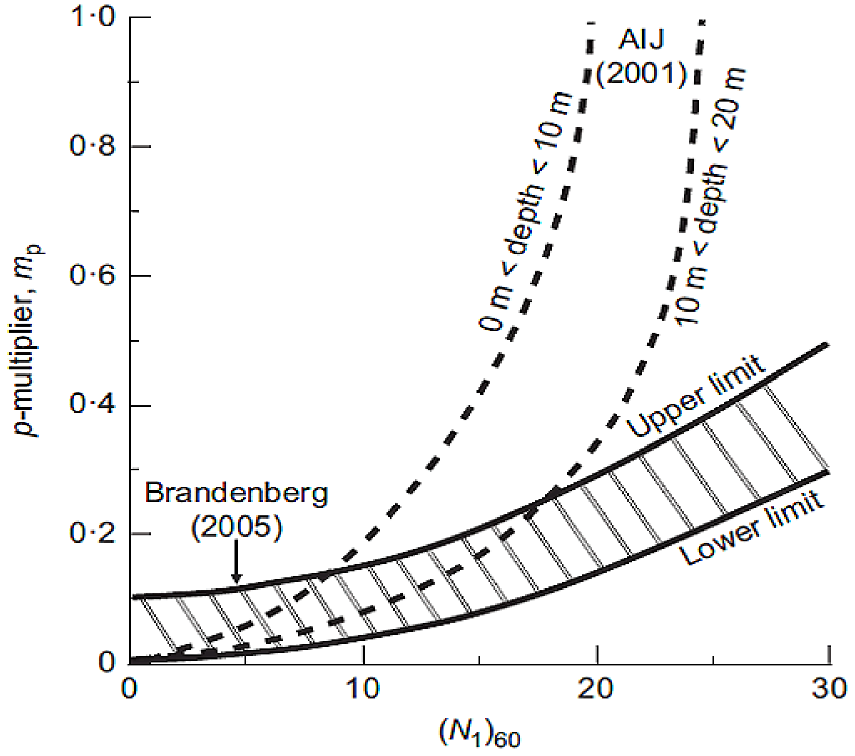

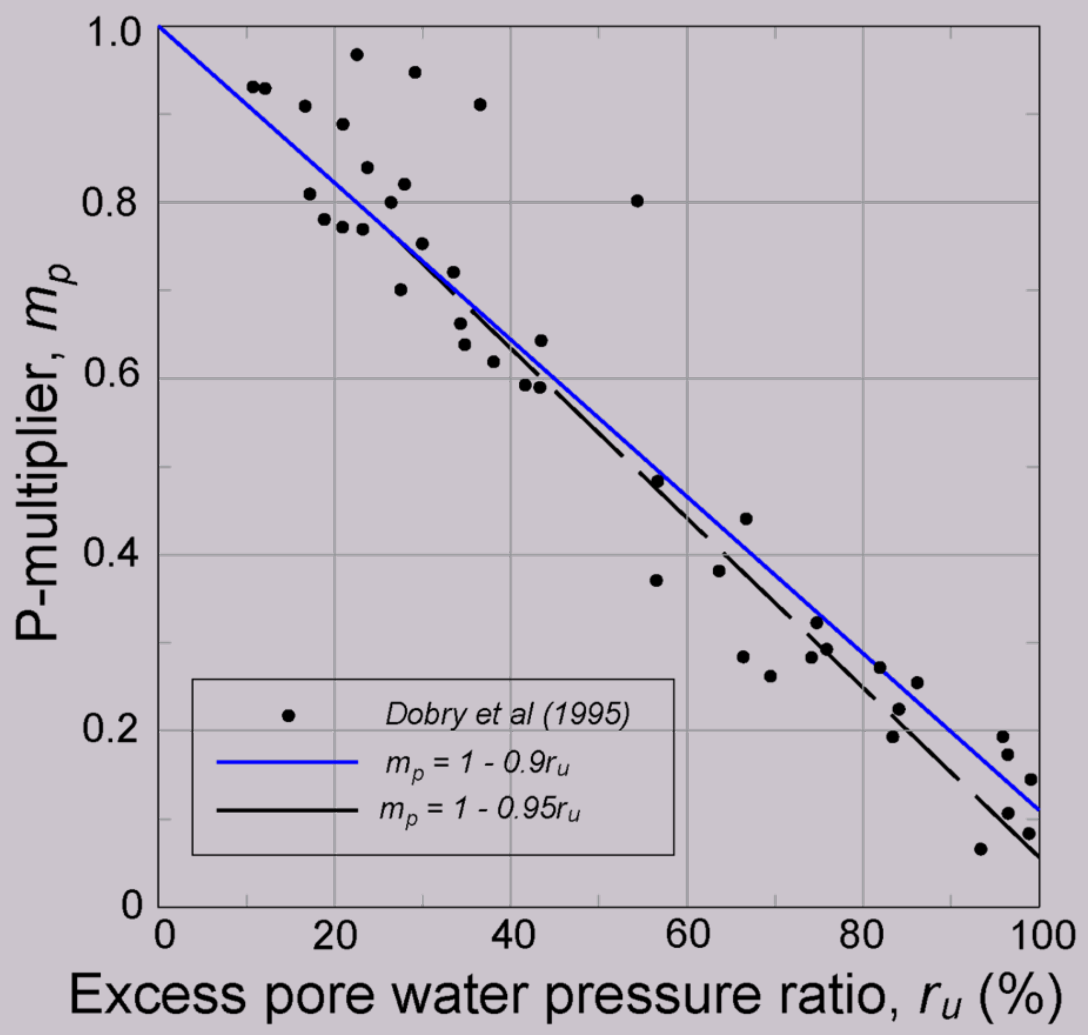

1.0
0.8
0.6
0.4
0.2
0
0
20
40
60
80
100
P-multiplier, m_p
Excess pore water pressure ratio, r_u (%)
Dobry et al (1995)
$m_p = 1 - 0.9r_u$
$m_p = 1 - 0.95r_u$